Int. J. Heat Mass Transfer. Vol. 7, pp. 447–478. Pergamon Press 1964. Printed in Great Britain

AN ATTEMPT TO MEASURE THE THERMAL CONDUCTIVITY OF LIQUIDS, GASES, AND VAPORS WITH A HIGH DEGREE OF ACCURACY OVER WIDE RANGES OF TEMPERATURE (−180 to 500°C) AND PRESSURE (Vacuum to 500 atm)†

W. LEIDENFROST‡

(*Received* 14 *October* 1963)

Abstract—A new thermal conductivity cell is described using a vertical cylinder with hemispherical ends within a similar cavity. The design and assembly of the cell and precautions to minimize errors are fully described. A high precision capacitance bridge was used to determine cell geometry. Dielectric property data was also therefore measurable. The thermostat design enables wide temperature ranges with low error to be obtained. A special pressure transmitter working at the test temperature is described. Detailed error analysis is made of losses along the centering devices and for convection and radiation. The first was eliminated with a new dimensionless number. Approximate and exact radiation losses are compared. The experimental accuracy is estimated at 0·1 per cent. Preliminary results are given for the dielectric constant of argon, carbon dioxide and toluene and the thermal conductivity of helium. Dielectric constant values agree within six parts per million with recommended data. The very small scatter from a smooth curve demonstrates the high accuracy of thermal conductivity values. Possible modifications are suggested to enable obtaining additional property values from a single determination, also of importance to statistical mechanical theories.

NOMENCLATURE

A_1, A_2, constants;
A_s, average cross-sectional area of the centering rod;
B, geometric constant;
C, electrical capacitance of the cell assembly;
C_e, capacitance with eccentricity in the arrangement;
C_o, capacitance with zero eccentricity in the arrangement or minimum capacitance in the arrangement;
c, velocity of light;
D, diameter of the cavity in the cold body;
D_a, D_i, diameters of annulus formed by test fluid surrounding the centering rod;
d, diameter of the heater element;
$E_{b,\lambda}$, monochromatic emissive power of a black body;
$E_n(x)$, exponential integral function, equation (18);
$E_{\lambda,i}$, monochromatic emissive power of surface i;
e, eccentricity;
Gr, Grashof number;
h, length of the cylinder of the combined configuration;
I, electric current;
K, dimensionless number;
k, thermal conductivity;
k_r, radiative conductivity;
k_s, apparent thermal conductivity of the centering rod;
L, length of the centering rod, also used as thickness of test layer in model for radiant heat exchange;
M, N, constants;

† The paper was presented at the 1963 Thermal Conductivity Conference at Gatlinburg, Tennessee, and was partly used also for discussion at the International Coordinating Committee on Properties of Steam at Providence, R.I.

‡ Professor of Engineering, Purdue University, Lafayette, Indiana, U.S.A.

m, coefficient;
n_λ, index of refraction;
Pr, Prandtl number;
p, pressure;
$\dot{q}$, heat generated per unit volume;
q_k, conductive heat flow per unit area and time;
q_L, heat loss from the heater element along the centering rod;
q_r, radiant heat flux;
R_h, resistance of the heater element;
$R_{i,\lambda}$, $R_{o,\lambda}$, monochromatic radiosity leaving the surface i and surface o, respectively;
R_L, resistance of the lead-in wires enclosed in the rod of length L;
r_i, r_o, distances;
T, temperature;
T_c, surface temperature of the cold body;
T_h, surface temperature of the heater element;
ΔT, temperature difference;
V, electric potential.

Greek symbols

β, variable;
ϵ, dielectric constant of substance;
ϵ_g, dielectric constant of gas;
ϵ_i, emissivity of surface i;
ϵ_o, emissivity of surface o;
ϵ_v, capacitance of vacuum;
ζ $= T - T_c$;
θ, variable;
κ_λ, monochromatic absorption coefficient;
κ_r, Rosseland mean free path of radiation;
μ, dynamic viscosity;
σ, Stefan–Boltzmann constant;
τ_λ, optical depth;
$\tau_{o,\lambda}$, optical thickness;
Φ, variable.

1. INTRODUCTION

THE rapid technological development during the last decades generated an increasing effort in expanding our knowledge of properties of materials. This seems to be especially true for transport properties since their exact values are needed whenever heat transfer must be evaluated and wherever the proper design of heat-transfer elements is as vital as in nuclear engineering, rocketry, space travel and in many other areas of our modern technology. The effort spent in experimental research as well as in theory has up to now not yielded the goal of predicting reliable data even for many common fluids and certainly not for newly developed working media applied at widening ranges of temperatures and pressures. It is hopeless to measure properties of all fluids even under moderate conditions; also it is impossible to determine them at such high temperatures where experiments cannot be carried out. But the need still remains; to meet the demand only one way seems feasible —this is a closer tie between theory and experiment. The theoretician should name to the experimenter the material to be investigated and the ranges to be covered. The experimental research in turn should try to measure property values with high precision and in ranges of temperature and pressure as wide as feasible for accurate measurements. If one property of one substance over wide ranges is accurately known then all effort should be spent to measure other properties of the same substance in the same ranges. Especially those other properties should be investigated which give, together with the first one, the most information to theoretical research on the estimation of intermolecular forces. Theoretical models for statistical mechanical treatment could then be proved and/or improved thus enabling the reliable calculation even over ranges where experimental observations are as yet impossible.

Since many properties change quite drastically with impurities one has to make sure that the tests are carried out with the same materials. To achieve this the best way would be to have instruments in which, for the same sample under identical conditions, different properties can be measured simultaneously. (This point will be discussed in more detail at the end of this paper.)

Next to the accuracy of the measurements and the quality of the sample the number of measured points is of importance. There should be not only a few data to cover a wide range but many

points on a curve in order to enable evaluation of gradients, change of gradients and inflections.

As recent surveys [1, 2] have shown, our knowledge of the thermal conductivity of gases, liquids and vapors is very incomplete or not in existence even at lower pressures and temperatures. Our investigation will try to fill in the gap, but much more important is the effort to measure the new data accurately and for this reason the paper will deal more with the instrument than with numbers of measured data.

This work had been initiated in 1958 when the author measured, with Kestin, the viscosity of several gases [3]. The high accuracy then achieved made it attractive for the above mentioned reasons to try to determine the thermal conductivity of the same substances in the same ranges with approaching accuracy. Besides this more scientific reason there also was a technical need for obtaining high temperature data for coolants in nuclear power plants [4]. The first sketch of the experiments made at Brown University had been followed up with a further design at the Forschungsinstitut für Verfahrenstechnik Aachen which finally led to a somewhat modified instrument now being used at Purdue University.

2. METHOD OF MEASUREMENT

It does not need to be discussed here that highly accurate measurements dictate an absolute steady state method. It is not as simple to decide which of the various known techniques should be used. The horizontal test layer heated from above and the, as common, coaxial cylinder arrangements both have the disadvantage of using guard heaters. The regulation of these increases the time needed to achieve steady state conditions considerably and there is furthermore the chance of undetected temperature fluctuations and connected with it a remaining temperature difference influencing heat flow from the main heater, not to mention the difficulties in heating uniformly, in alignment and in insulating and sealing the guard heaters especially over wide ranges of pressure and temperature.

Guard heaters and the difficulties they introduce can be avoided by using arrangements where the heat source is completely surrounded by the test material and the heat sink, which can be done only by producing heat by an exothermal process within the source at a given temperature. The more common arrangement uses electrical heat input and the temperatures of the heat source are measured by thermocouples or resistance thermometers; therefore the heat source cannot be surrounded completely since part of the available heat flow area must be occupied by lead-in wires. This introduces errors but they can be made very small as will be shown later.

At a first glance the spherical arrangement appears to be the best but this geometry has the disadvantage that a spherical heater producing uniform heat flux is difficult to fabricate. Furthermore the influence of eccentricity on the accuracy of the measurements is only a function of the eccentricity itself and not of the direction of eccentricity. This means the spheres exactly centered along one axis gives no advantage if eccentricity exists in the other axis. Whereas with a cylindrical arrangement, especially when the length to diameter ratio is large, it is less important to have equally thick layers at the ends when the axial adjustment is correct, since the heat-transfer areas of the ends are small compared with that of the annulus. Of disadvantage on the other hand is the thermal inhomogenity at the cylinder ends which again introduces problems in producing a uniform heat flux for the sake of temperature uniformity which is also essential to keep free convective heat transfer at a minimum.

The drawbacks of the spherical and cylindrical annuli can be decreased or avoided by using a combined arrangement for which most of the advantages of the two configurations can be maintained.

Cylindrical heater elements with hemispherical ends placed within an equally shaped cavity of a cold body acting as a heat sink was first used by Schmidt and Leidenfrost [5]. In this paper, and in other investigations with modified instruments [6, 7], detailed information is given and especially the ease and speed of operation and the accuracy are demonstrated and discussed. Therefore only specific features of the new thermal conductivity cell need to be presented here.

3. EXPERIMENTAL

3.1 *The conductivity cell*

A cross section of the cell is shown in Fig. 1. The heater element (1), completely enclosed by the cold body (2), is centered at its base by means of a small thin walled tube (3), and at its upper end by a long centering rod (4), in which all lead-in wires to the heater element are enclosed. The gap (5) between the heater element and cold body of nominal 0·05 cm width is, for the test, filled with the fluid. For measuring gases and liquids, charging the cell is done through the tube (6) connected to the instrument at the bottom. If vapors are to be tested, liquid will be brought in at the top where in the figure the seal (7) is shown now. The centering rod passes through the cold body in order to suspend the cell from the top closure of the high pressure vessel (8) with least thermal conduct. This high pressure vessel itself is completely immersed in the water bath maintained at tap water temperature.

In operation the cold body is heated or cooled and maintained at the required temperature and the heater element is heated electrically by such an amount that equilibrium is reached at a temperature difference small enough to avoid free convection and to minimize radiant heat transfer but large enough to be detectable with a high degree of accuracy. The temperature difference across the gap, the heat input, together with the geometric constant of the system enables the calculation of the thermal conductivity to be made.

The cold body and the heater element are made of high purity copper. The low strength of this material especially at high temperatures made it necessary to follow special precautions in order to avoid damage to the cell under pressure which might cause a change in the geometry and therefore influence the accuracy of the investigation. The forces acting on the inner surface of the cold body under the test pressure is balanced by equalizing the pressure of the gas in the high pressure vessel surrounding the cell. This simple balancing cannot be done easily in the case of the heater element because its interior is, for construction reasons, connected to the atmosphere. Fig. 2, representing a cross section of the heater element, shows the precaution followed to avoid damage under pressure. In the axis of the heater element is placed the electrical heating coil (1). Three 1 mm

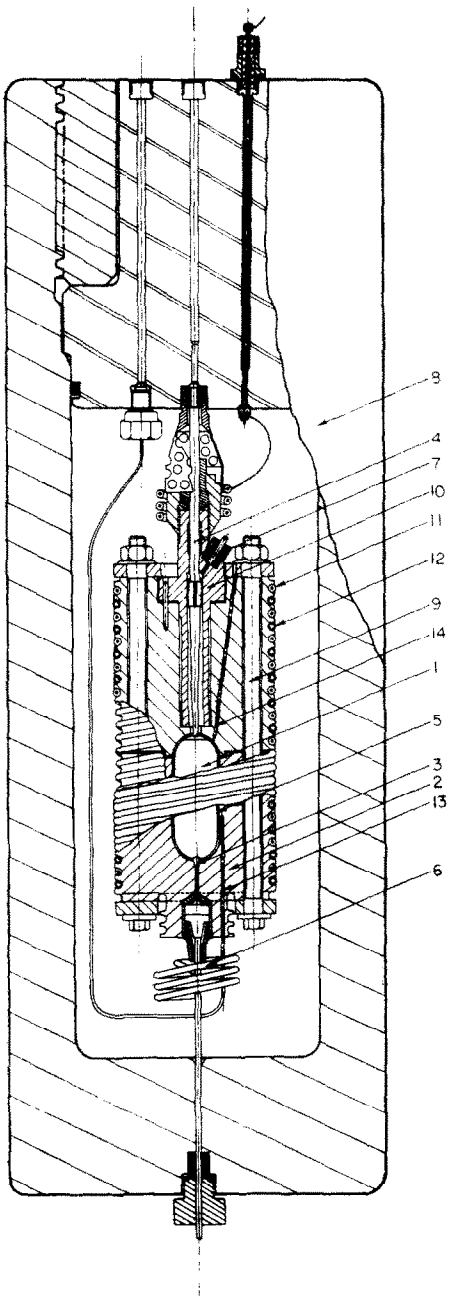

FIG. 1. Thermal conductivity cell enclosed in high pressure vessel.

holes (2) accommodating the thermocouples are equally spaced on the circumference and drilled at different angles so deep that they terminate at different heights within the heater element and 0·5 mm away from its surface. Due to the small diameters of the holes protection against pressure is needed only at the ends which is done by filling the holes there tightly with copper tips (3), in which also the thermocouple wires are jointed together for the hot junctions. The bore for accommodating the heating coil weakens the heater element most and therefore it was necessary to fill it solidly and completely with least possible clearance and by making sure that the thermal expansion of the coil is equal that of copper. This necessity is achieved by winding the electrical wires (4) enclosed in a 0·5 mm diameter stainless steel tube on a copper rod (5) and hard soldering this combination into a copper tube (6) by using a solder which has almost the thermal expansion coefficient of copper. The opening at the top of the heater element is relatively large for making, machining and drilling of the thermocouple holes possible. This large opening brings the disadvantage that the forces acting on the base (7) of the centering rod might at high temperatures exceed the strength of copper at the small supporting rim. In order to avoid deformation the rim is strengthened by three fine threaded screws (8) made out of a steel chosen to have the same thermal expansion as copper.

To seal the conductivity cell special care must be also taken to prevent damage and deformation of the copper material. To seal the heater element an O-ring made out of pure gold wire is used. This O-ring with an outside diameter equal the diameter of the hole is, by means of the ring nut (9) acting on a sleeve (10), squeezed into its final shape (11) filling the gap between the sleeve, the outside wall of the bore and the base of the centering rod completely. Selecting the diameter of the gold wire properly guarantees a foolproof seal under fluctuating temperature and pressure conditions and prevents damage of the copper wall.

A similar arrangement is used to seal the opening where the centering rod passes through the cold body. As seen in Fig. 1, the cold body is subdivided at the upper end of the cylindrical part of its cavity. To seal the cold body here a gold O-ring is used.

To avoid welding of the gold with the copper a nickel coating as a diffusion barrier is necessary.

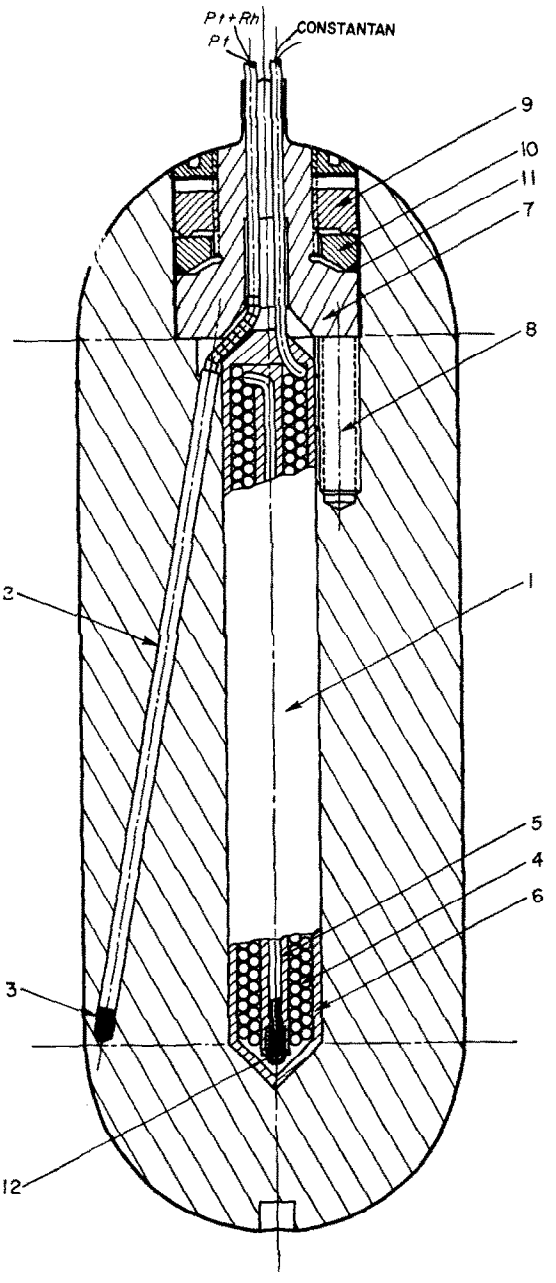

FIG. 2. Heater element.

Since the pressure acting on the inside walls of the cavity of the cold body is balanced by equal outside pressure, the two parts of the cold body need to be held together only so tight that sealing of the test fluid is assured. The sealing force is applied by means of eight bolts (9) as shown in Fig. 1. These bolts are made out of a special high temperature steel of the same thermal expansion as copper. Therefore, the sealing force acting on the cold body remains constant for all temperature ranges. This force is high enough to assure a definite seal but low enough that the copper is not deformed even at high temperatures.

3.2 *The geometric constant*

The heat flow conducted in steady state through a fluid layer of the form of a cylindrical annulus with hemispherical ends can be given by

$$q_k = k\,(T_h - T_c)\,2\pi\left(\frac{h}{\ln D/d} + \frac{D \cdot d}{D - d}\right) \quad (1)$$

where h is the length of the cylinder of the combined configuration; D and d are the diameters of the cavity in the cold body and of the heater element; T_h and T_c are the respective surface temperatures of the two bodies.

This simple equation holds true under the assumption that only radial heat flow exists. But in the combined arrangement there certainly exists a thermal inhomogeneity at the transition from the cylindrical to spherical portions of the annulus due to the fact that at this point the temperature profile across the gap changes from a logarithmic to a hyperbolic one. This error can be made very small by proper choice of diameter and gap width. Direct measurements of the diameters and the cylinder height prove to be extremely difficult. More reliable results are obtainable by determining the volumes of heater element and cavity of the cold body. But even with this method quite an uncertainty remains since both observations can yield the dimensions only by solving cubic equations and matching one result with the other; i.e. for equal length of the cylindrical part. No matter how carefully one operates and how sensitive are the instruments one uses it is impossible to determine the geometric constant exactly because surface roughness cannot be accounted for and furthermore there exists the above mentioned unhomogeneity and also other disturbances of the temperature field at locations like the top and bottom holes in the cold body and heater element and at the place where the two parts of the cold body are joined together with a small gap in-between. For our symmetrical arrangement the increase in heat flow area due to those effects could be estimated by conformal mapping. But only to a certain degree of accuracy since this analysis depends on the knowledge of the geometrical dimensions and configurations of these disturbance points. The most promising way to determine the geometric constant is to measure the electrical capacitance of the cell assembly, because due to the similarity between the electrical and thermal field all unhomogeneities will be included. The capacity measured will be

$$C = \epsilon_v \cdot \epsilon_g \cdot B. \quad (2)$$

Measuring under vacuum makes the dielectric constant $\epsilon_g = 1$ and the geometric constant becomes

$$B = \frac{C}{\epsilon_v} \quad (2a)$$

where the capacitance of vacuum

$$\epsilon_v = \frac{1}{4\pi c^2}\,10^7 = 8{\cdot}8541735 \times 10^{-10}\,\frac{\text{Farad}}{\text{cm}}$$

when the velocity of light $c = 2{\cdot}997927 \times 10^8$ m/s.

The geometric constant B measured electrically is of value for the determination of thermal conductivity only if in both measurements the same eccentricity exists or none at all. As described in Section 3.1 the heater element is centered definitely at the bottom by means of a small tube and at the top by the long centering rod. The centering rod places the axis of the heater element not only on the axis of the cavity it allows also the heater element to be located in its proper position axially by screwing it on a fine thread into the upper end of the tube (10) soldered to the cold body as shown in Fig. 1 (this screw connection is necessary also for the purpose of suspending the cell from the top of the high pressure vessel).

The centering rod has furthermore to fulfill the requirement of conducting as little heat away from the heater element as possible which is assured by making the rod very thin walled at its lower end. This in turn requires the use of a material of high strength at high temperature. The high nickel alloy "Nimonic" suited the needs best also in respect to its low thermal conductivity and its high chemical resistance. Since Nimonic has a different thermal expansion coefficient than copper a compensation device is needed to keep the heater element at all temperatures in its proper position, for this reason the tube (10) is used. Since this tube could not be made as long as the centering rod a differently alloyed Nimonic is necessary to assure compensation.

Further assurance for proper placing of the heater element within the cavity is given by shimming the two parts of the cold body which avoids a change in the total height of the cavity under differently applied sealing forces.

During the measurements of the geometric constant the centering devices are replaced for electrical reasons by geometrically identical ones. The centering rod described above is replaced by a tube which acts as extension of the guard of the electrical lead to the heater element. This centering tube is also insulated at its outside along the length of its passage through the cold body. This arrangement allows three lead capacitance measurements and the capacity of the cell assembly can therefore be obtained by direct readings; the lead-in capacities have no effect. The instrument used is a newly developed capacitance measuring assembly made by General Radio Company (Type 1620-A, accuracy 0·01 per cent from 1 pF to 1 μF).

If one assumes perfect alignment of the axis of the heater element and the cold body cavity, the capacity of the arrangement depends only on its location along the axis, and must have a minimum value where the least fringe effects are present. At this location the temperature field is most uniform and it is therefore of advantage to place the heater element in this position. In order to find this point it is necessary to determine the capacity curve as a function of vertical displacement, which in our case could be done easily by means of the screw arrangement. The results of the measurements are given in Fig. 3. The upper plot gives the total change of capacity by moving the heater element from its uppermost position (being in contact with the cold body at the top) to its lowest location (touching the cold body at the bottom). The displacement is given in terms of degrees of turning on the fine thread with 0·5 mm lead and also in terms of axial motion. The total movement is achieved by turning the centering tube 750°. Due to the opening at the top and bottom of the cold body the heater element could be moved in either direction a little further. The geometrical contact, where the upper hemisphere of the heater element would touch the upper hemisphere of the cold body therefore is at 15° and similarly at the bottom at 748°. The curve, measured several times in either direction, indicates a minimum value of the capacity at 317° from the physical contact at the top. The minimum does not occur at the geometrical center which is due to the fact that the relatively large opening at the top decreases the capacity. Since in the upper part more disturbance of the field exists the capacity changes with eccentricity more significantly than at the lower end. In Fig. 3 is also shown the section of the curve in the neighborhood of the minimum magnified one-hundredfold. The overall scatter of the measured points in the curve is of the order of thousandths of a per cent. The larger scatter to be noticed at the not enlarged curve is partly due to misreadings on the fairly coarse degree dial used (which is of less effect at minimum setting) and, especially at the bottom end, is caused by surface roughness of the thread and by axial play in the screwing arrangement, which causes by reversing the motion, an axial shift due to the friction in the O-ring seal changing contact from one flange of the thread to the other.

To allow further analysis of the readings the measured data are replotted in Fig. 4 as curve (4). In Fig. 4 the capacities are made dimensionless with the minimum value. For comparison the capacity as function of eccentricity is given for other geometrical arrangements; infinitely long cylinders (1) spherical (2) and for a combined arrangement where eccentricity exists only in the spherical part (3). The curves (1), (2) and (3) are calculated with the equations:

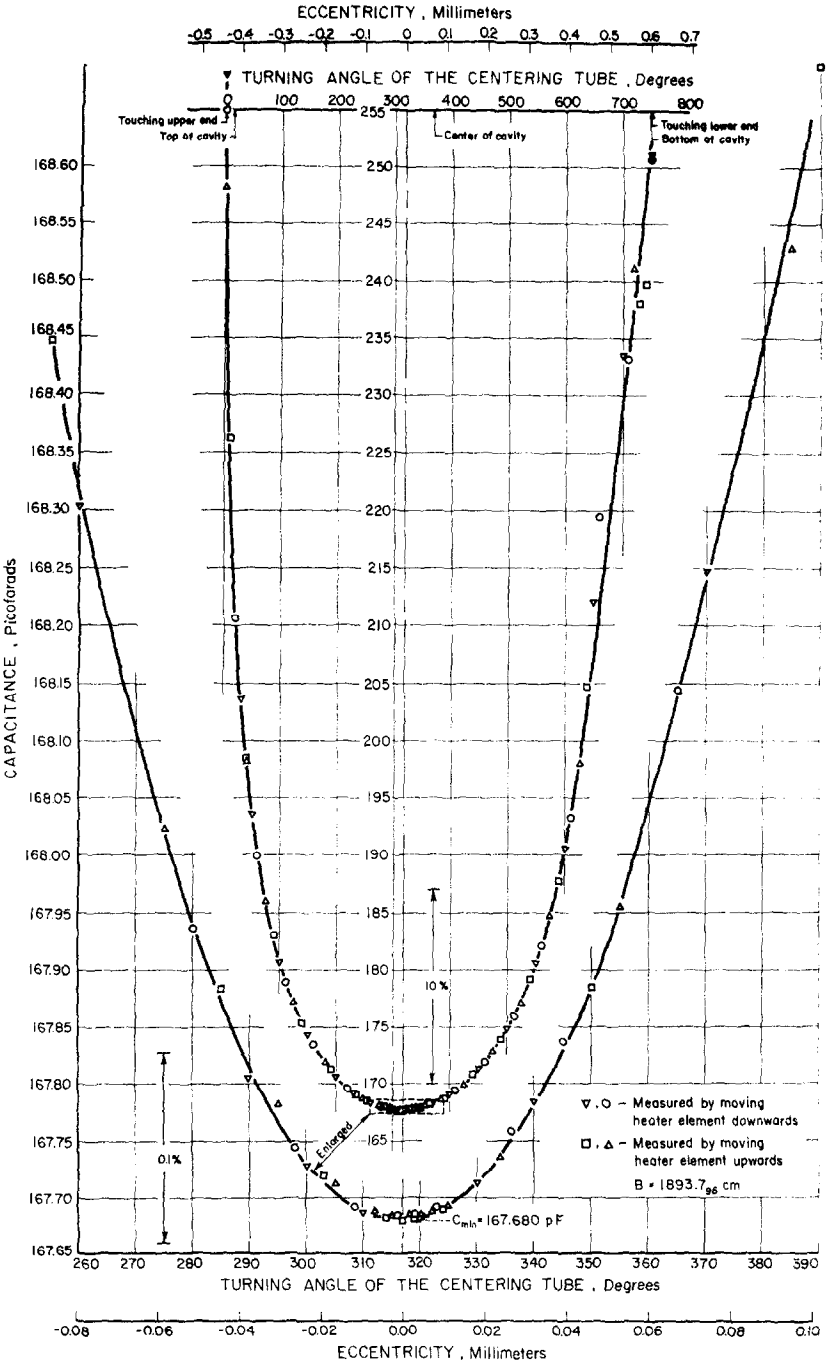

FIG. 3. Measurement of the geometric constant, *B*.

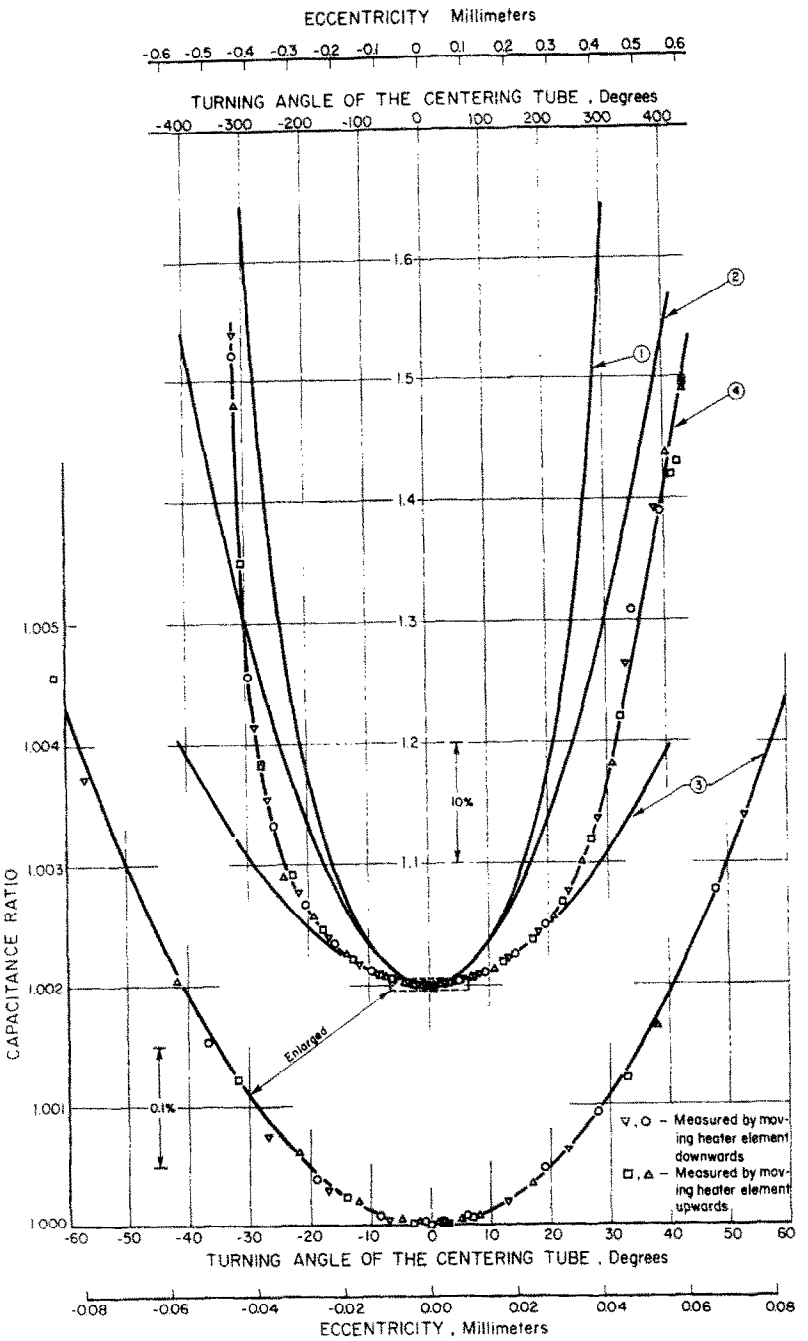

FIG. 4. Comparison of measured capacitance ratio with theoretical curves of some other geometric configurations.

For cylindrical arrangement

$$\frac{C_e}{C_o} = \frac{1}{\sqrt{\left\{1 - \left[\frac{e}{(D/2)\ln(D/d)}\right]^2\right\}}}. \quad (3)$$

For the spherical arrangement, neglecting higher order terms,

$$\frac{C_e}{C_o} = 1 + 2\left[\frac{d}{D(D-d)}\right]^2 e^2. \quad (4)$$

For the combined arrangement

$$\frac{C_e}{C_o} = \frac{(C_e)\text{ sphere} + (C_o)\text{ cylinder}}{(C_o)\text{ sphere} + (C_o)\text{ cylinder}} \quad (5)$$

where e = eccentricity. Since the diameter d of the heater element and D of the cavity are known only nominally it was necessary to determine them more accurately and to vary them together with the height of the cylindrical portion so that they give, using equation (1), the measured minimum capacity. For this purpose the diameter and the total height of the heater element were measured carefully and the total travel length of the heater element within the cavity, after correcting for the additional movements at the top and bottom, was equalled to $D - d$. The curve (4) in Fig. 4 shows the same trend as was seen in Fig. 3 but the different dependence of the capacity on the eccentricity in the upper and lower part is more noticeable. Furthermore, the severity of the fringe effects is demonstrated. The result shown more clearly in the hundred times magnified portion of the curve (3) is very satisfactory. The excellent fit of the measured points on the curve indicates that the axis of heater element and cavity had been aligned nearly perfectly. Of further significance is the fact that, for vertical displacements of 0·15 mm in either direction, the measured curve still coincides with the theoretical one of the combined arrangement. The measured points scatter around the theoretical curve only by a few thousandths of a per cent. Since during the assembly of the instrument all dimensions but one (that of the centering rod) are fixed, it is demonstrated by the calibration that the originally determined value of the geometric constant will be always obtained within 0·01 per cent because errors of this order occur at displacements of some $\pm 10°$ which is unlikely to happen. This was proven by excellent reproducibility of the results. The most uniform field will be achieved as already mentioned at a displacement 317° from the top (and not at the geometrical center at 381°). The upper spherical gap is therefore less wide than the lower one which has the advantage of minimizing free convective heat transfer.

In the present arrangement the geometric constant could be measured only at room temperature. The change with temperature, (approximately 0·17 per cent per 100°) can be calculated precisely enough with the well-known coefficient of thermal expansion of copper. Pressure effects on the geometric constant can be neglected because of the low compressibility of metals.

3.3 *Thermostat arrangement*

In order to gain the advantage of easy and fast temperature regulation the cold body itself as shown in Fig. 1 is designed as a thermostat. It is heated directly by means of electrical coils (11) wound bifilarly on the upper and lower parts. The two heaters are only needed to heat the cold body rapidly to the required temperature and to compensate for all heat losses to the pressure vessel, which are minimized by a multi-layer of radiation shields surrounding the cell. From the upper part of the cold body many connections are made to the top closure of the high pressure vessel which made it necessary to heat the two heater coils separately.

To avoid the influence of room temperature fluctuations the high pressure vessel enclosing the conductivity cell is kept at a constant temperature by means of a water bath [Fig. 5 (2)]. The other part of the thermostat is a cooling coil [Fig. 1 (12)] placed between the windings of the heater. Through this coil air is forced. The air passes first through another coil [Fig. 5 (3)] placed within the water bath to assure constant inlet temperature. The air within the coil of the thermostat flows bifilarly, its average temperature along the cold body therefore will be constant contributing to temperature uniformity of the cold body. By changing the inlet pressure the cooling effect can easily be regulated. Heating

of the coils is done by batteries or a constant voltage power supply with the aid of a control system. Previous experiments have shown that such a thermostated cold body is heated uniformly and is able to keep the temperature constant for a long time. Also, changing the temperature level for successive tests can be achieved quickly. This means that the steady state needed for the measurements can be rapidly reached and constant temperatures readily and accurately maintained.

For measurements at temperatures somewhat lower than room temperature the coil in the water bath is bypassed and the air becomes pre-cooled in liquid nitrogen. For even lower temperatures a refrigerant or liquid nitrogen will be forced through the cooling coil.

3.4 *Temperature measurements and thermocouple calibration*

All temperatures are measured with Pt–Pt 10% Rh thermocouples by using an ice bath or a triple point cell as reference. The emf's of the couples are measured with a 6-dial Rubicon potentiometer and a high sensitive electronic null detector able to make 0·01 μV visible. This refers to a temperature change for these thermocouples of approximately 0·0017 degC. There are three thermocouples evenly placed on circumference and height of the heater element as already shown in Fig. 2 (2) and three thermocouples are placed in the lower part of the cold body at opposite locations, Fig. 1 (13). A fourth thermocouple, Fig. 1 (14), measuring the temperature of the upper part of the cold body, is located at a similar location close to the spherical surface as the thermocouple placed lowest in the heater element. This fourth thermocouple is needed for proper adjustment of upper heater coil of the cold body and can also be used for recalibration. The legs of the thermocouples are joined together by electrical discharge welding. In order to assure good thermal conduction at a known location the joint is wedged into a small hole of a copper tip which fits tightly into the bore provided. In order to avoid contamination and physical damage the wires are insulated with high purity twin-bore alumina tubing placed within a stainless steel tube. To minimize influences of inhomogeneities which might have been introduced during the welding process the thermocouples are, whenever possible, guided a long distance along an isotherm. The stainless steel tube is hard soldered to the copper tip, therefore sealing the thermocouple at the hot junction. The tubes are bent gently, as seen in [Fig. 1 (13)], in such a way that spring action remains forcing the tip into good thermal contact. All thermocouple wires are outside the high pressure vessel connected to pure copper wires leading to the emf-free thermocouple switch. To assure

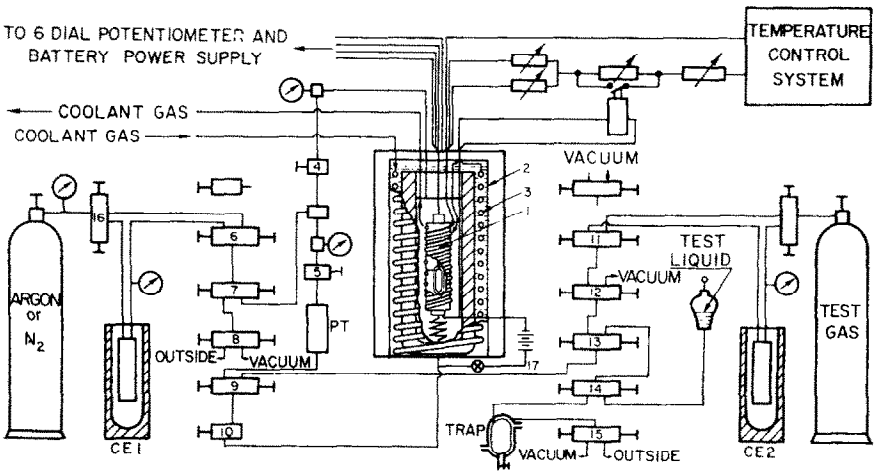

FIG. 5. Layout of experimental setup.

temperature uniformity of all connections the junctions are enclosed in a heavy brass block placed within a Dewar. Normal room temperature fluctuation will therefore never reach the joints, and continuous change of temperature will also be of no influence on the uniformity. The thermocouples leading from the top closure of the high pressure vessel to the junction Dewar are rigidly mounted to avoid bending. For the same reason the Dewar and the cold junction are fastened to the top closure of the high pressure vessel in such a way that they keep their position whenever the instrument is moved.

The calibration of the thermocouples is performed in a stainless steel cylinder in which a temperature uniformity of 0·001 degC could be maintained at any temperature level due to a thermostating arrangement like that of the cold body. A hole along the axis of the cylinder accommodates a calibrated platinum-resistance thermometer. Three out of the seven thermocouples used in the conductivity cell were placed in holes drilled on a circle around the resistance thermometer. The calibration curve was obtained by repeated measurements in such a way that there was in the whole range (at about every 20°C), a calibration point. The gradients of this curve plotted versus emf made graphical interpolation possible, in addition the emf–temperature relation was represented by an equation. All thermocouple wires had been selected for homogeneity and for this reason together with proper annealing emf readings between individual thermocouples differed only by negligible small amounts or could not even be observed. The thermocouples can easily be checked when they are mounted in the apparatus and no heat is generated within the heater element. In this way the four uncalibrated couples have been tested with excellent results.

3.5 *Heating the heater element and measuring the power input*

The cross section of the heater element in Fig. 2 shows also the electric heater coil in detail as discussed in Section 3.1. The coil is fitted by a lapping process into the hole accommodating it. This tight fit has, besides being able to withstand high pressure, the advantage of assuring good thermal contact. The bifilar windings of the coil are in the center less close than at the ends in order to assure uniform heat flux at any location of the heater element surface. The coil itself consists of chromel–alumel thermocouple wires placed inside a 0·5 mm stainless steel tube insulated by magnesium oxide. At the lower end of the coil the two wires are joined together by a constantan wire (12) and constantan wires also extend the chromel–alumel leads at the top. This serves three purposes. First, any thermal emf of the chromel–alumel heater wires is cancelled out and will therefore not influence the power measurements. Secondly, the heat loss along the copper lead-in wires to the heater element is minimized and finally the constantan wires act as heaters to correct for heat loss along the centering rod, as discussed in more detail later.

The heat dissipated in the coil is determined by measuring the current and the voltage with the aid of standard resistors and the six dial potentiometer. To correct for the voltage drop along the lead-in wires, their resistance has been measured at room temperature carefully with a high precision Wheatstone bridge. Since the lead-ins consist of different wires of different length and can undergo different temperature changes it is necessary to measure each individually so that the true overall lead-in resistance can be calculated for temperature changes. This also is of importance for evaluation of the heat loss along the rod.

3.6 *Filling and emptying the cell, pressurizing the test fluid and the gas in the high pressure vessel and measurement of the pressure*

The discussion easily can be followed from Fig. 5, showing the layout and experimental set-up.

When liquids are to be measured the glass apparatus containing the gas-freed test fluid is connected with the bottom of the conductivity cell (1) and, a pressure transmitter and expansion chamber (PT) which is shown in Fig. 6. There it can be seen that it is connected at the top with the high pressure vessel surrounding the conductivity cell and at the bottom with the gap of the cell itself. During the measurements the test liquid fills the inner tube (1) and part of the

annulus formed with the outer tube (2). The test fluid is separated from the gas pressurizing the high pressure vessel by mercury which fills the lower part of the annulus and part of the annulus (3) which is connected to the first one by several holes drilled radially through the wall of tube (2) at its lower end. At any measuring conditions the pressure of the test fluid is by this arrangement practically equal that of the pressure acting on the outside of the cold body. The pressure of the gas is measured by a calibrated Bourdon-type gauge which can be replaced by a pressure balance. Since the influence of pressure on the thermal conductivity of liquids is small, the readings with the gauge are accurate enough and there is also no need to correct for small pressure differences introduced by the imperfectly matched levels of the different liquids within the unit. Temperature changes in the test cell will cause only a displacement of the level of the test fluid within the annulus between (1) and (2). The dimensions have been chosen to fit any possible volume change of a liquid from freezing to critical point conditions. This dimension had to be correct furthermore also in respect to the mercury for the following reason. This annulus (3) together with the amount of mercury used had been designed so that under no circumstances mercury ever can reach the gap within the test cell, even when the test fluid is removed completely by accident. In this case the gas of the high pressure vessel can bypass the mercury and fill the gap of the cell.

The safety device necessary to protect the gold coated walls of the test cell necessitates filling the instrument in two steps instead of one. The steps can be followed from Fig. 5. First step, with valves (4) (10), (11), (14) and (15) closed, unit (PT) and all connecting tubes are evacuated by means of valves (8) and (12) making possible the evacuation of each leg of the mercury U-tube arrangement. After closing valves (5) and (12), valve (14) is opened to connect the liquid reservoir to the system. Under atmospheric pressure all lines are filled and the mercury fills annulus (3) in Fig. 6 completely. Valves (5) and (15) are opened now to the atmosphere causing part of the liquid to drain into (trap) until the forces acting on both limbs of the mercury are balanced. Annulus (3) Fig. 6 is now only partly filled with mercury allowing the second step and expansion of the test fluid during the measurements.

During the filling of the cell itself the connection to unit (PT) is shut off by means of valve (9), valve (10) is opened and the instrument becomes filled with the test liquid under vacuum in a self-explanatory way. In order to assure gas free operation the instrument is filled and emptied several times and, if necessary, by cycling the temperature of the conductivity cell. During the test valves (8), (11), (12), (13), (14), and (15) are closed and valves (4), (5), (6), (7), (9) and (10) remain open. To increase the pressure of the test fluid to around 120 atm commercial argon or nitrogen bottles are connected with the instrument by means of valve (16). For operation under higher pressures up to the limit of the instrument the bottled gas is compressed first with the aid of a diaphragm type compressor or by a condensation and evaporation process in unit (CE1).

In measuring gases, unit (PT) is not used and is kept out of operation by closing valves (5) and (9). Also not needed are liquid reservoir and (trap). The test gas stored in a bottle is, as shown in the layout, either directly connected with the cell or is first passed through unit (CE2) similar to unit (CE1) needed to increase the pressure above storage tank pressure by avoiding contamination. This unit also will be used to empty the cell by a condensation process in cases where the test substance must be recovered completely. Since the pressures acting on the outside and inside of the cell are not balanced automatically an additional calibrated gauge is connected to the test side (not shown in the layout).

For measuring vapors, the test cell originally filled with a certain amount of liquid is completely closed. There are no open connections to the outside in order to avoid condensation which would cause, due to the small volume of the cell, a rapid pressure decrease which could produce damage to the instrument when the outside pressure cannot be lowered fast enough. In order to measure the vapor pressure part (6) in Fig. 1 is replaced by a membrane-operated device working at test temperature. Fig. 7 shows this device in detail. It consists of an upper part

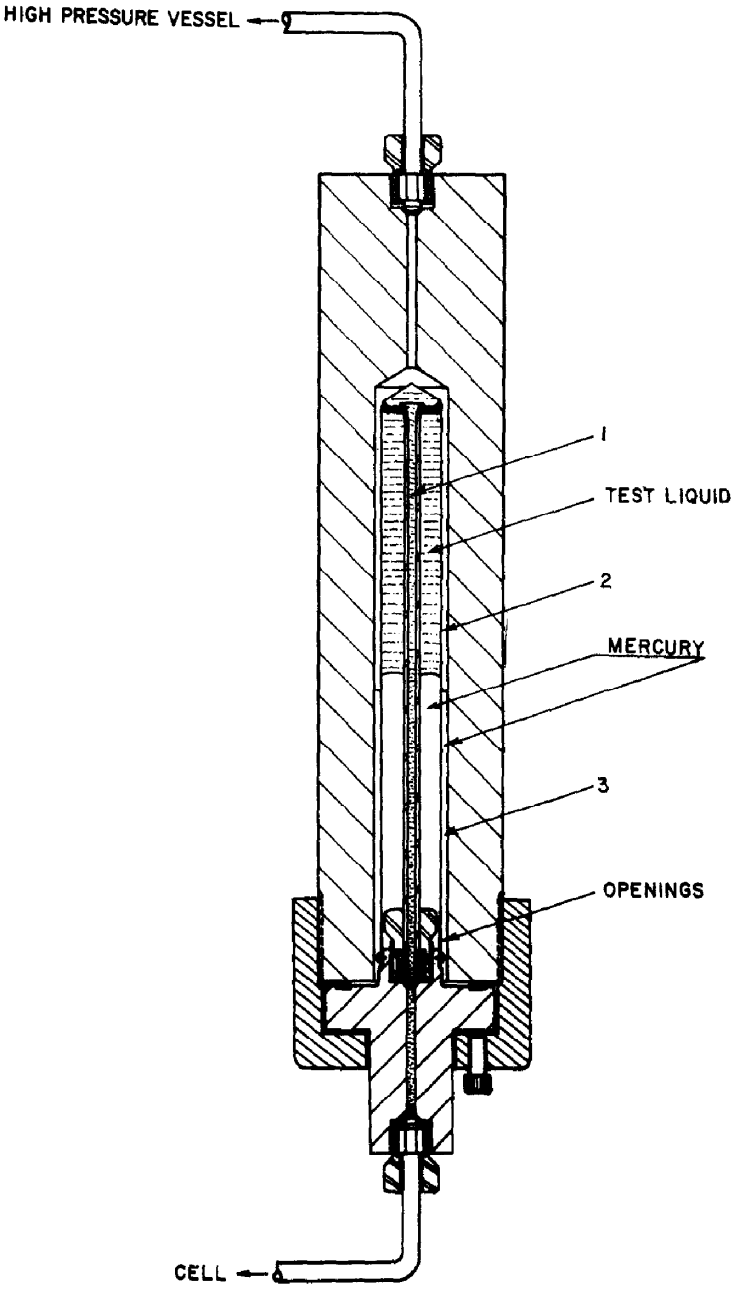

FIG. 6. Pressure transmitter and expansion chamber.

(1) shaped at its top to act as a high pressure seal under the action of a ring screw (2) and a lower part (3) which encloses in its center an electrically insulated part (4). Parts (1) and (3) and a thin walled membrane made out of a gold alloy in-between them are at the same time joined together by silver solder. The upper surface of the membrane is in contact with the vapor tested and its lower surface in contact with argon or nitrogen gas pressurizing the high pressure vessel. If the vapor pressure is higher than the gas pressure the membrane is pressed against the surfaces of part (3) and (4) (being flat and in the same plane) assuring the closing of an electrical circuit as indicated in (17) of Fig. 5. If the pressure on the other side of the membrane is higher than the vapor pressure the membrane will buckle and break the electrical circuit. The membrane obviously will not be damaged no matter how much the vapor pressure exceeds the gas pressure. To assure similar strength under the opposite conditions buckling of the membrane is limited by a nickel sieve (5) built into part (1) and formed into proper shape. Holes in the sieve of 0·001 mm diameter are large enough to assure free passage of the vapor but far too small to cause damage to the membrane as was proven by tests at 500 °C and 500 atm pressure difference. The small thickness of the membrane and the soft material used makes the device sensitive enough for thermal conductivity measurements.

Since the thermal expansion coefficient of the membrane material is not perfectly equal that of the materials used for part (1) and (3) the sensitivity changes somewhat with temperature

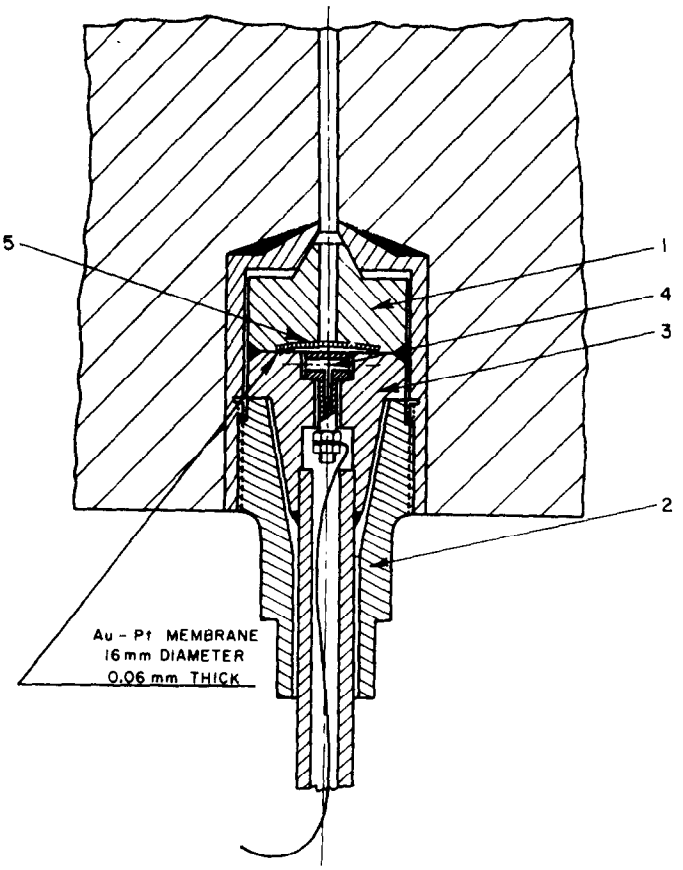

FIG. 7. Device for measuring vapor pressure.

but it is always better than 0·1 atm. Another advantage of the pressure measuring device is that the thermal conductivity cell by measuring vapors can be regarded as a constant volume instrument.

To assure reliable and reproducible results all substances measured will be tested for purity before and after the measurements; for this reason arrangements are made to collect the test fluid whenever the instrument is emptied. Fig. 8 shows the total arrangement. The high pressure vessel and the water bath are enclosed in the main unit shown in the center of the photograph. All valves and gauges needed for operation are attached to this unit and located in a similar way as in Fig. 5. The top closure of the high pressure vessel with the cell attached, the thermocouple junction Dewar and the cold reference container are suspended from a screw which can be moved up or down by means of an electric motor. To the rear on both sides of the main unit can be seen the two units needed for pressurizing the gas in the pressure vessel and the test fluid. At the right-hand side is seen the instrumentation for measuring emf's of thermocouples and the power input to the heater element. (Similar units had been used extensively at the technical universities Braunschweig and München and at the Forschungsinstitut Verfahrenstechnik Aachen. They proved their high reliability due to their perfect shielding.) At the left side is the AC-DC power unit for heating the cold body of the cell. All units are mobile and can therefore easily be moved whenever they should be used for other purposes. The unit enclosing the six dial potentiometer is for the same reason easy to disconnect and furthermore provisions are made to connect other circuits without introducing disturbances. The arrangement of the total instrumentation is in easy reach of one individual for reading and controlling and therefore the experiments can be carried out by one man.

3.7 *Sources of errors and corrections*

With the geometric constant B, equation (1) can be solved for k

$$k = \frac{V \cdot I}{\Delta T \cdot B} \qquad (1a)$$

where $V \cdot I$ is the electrical power input to the heater element.

As proven in Section 3.2. B can be assumed to be accurately known within 0·01 per cent. A similar accuracy can be achieved in measuring the power input and emf's of the thermocouples. This does not mean that the thermal conductivity evaluated with those measured quantities will be as accurate due to several facts. First, the temperature difference measured at locations somewhat below the surfaces of heater element and cold body is not equal to the ΔT of equation (1a) due to temperature drops in the walls. Secondly, the heat generated within the heater element is not only, as the equation demands, transferred to the cold body by conduction through the layer of test fluid but also is conducted along the centering devices and furthermore, transferred by convection and radiation. All these errors are functions of ΔT and also complicated functions of the geometry of the system and of the thermal conductivity measured and many other properties involved. In addition, the errors are functions of pressure and temperature. From all this it becomes clear that achieving a fair accuracy in thermal conductivity measurements one has first to reduce the sources of errors. Remaining errors must be small and they should be either detectable by measurements or analytically with sufficient precision. Normally changing the experimental conditions to eliminate one error can make others larger, therefore compromises are necessary. This increases the effort considerably and also the time required in a process which is inevitably slow if high precision is attempted.

3.7.1. *Heat flow along the centering tube and the centering rod.* The centering tube of 3 mm outside diameter, holding the heater element at the bottom in place, is very thin walled and made of poor conducting high nickel alloy. Its cross-sectional area occupies only 0·003 per cent of the overall heat flow area. To minimize the heat flow further there are many holes drilled in a staggered arrangement through the tube wall at the location where it bridges the gap between heater element and cold body. The very small amount of heat flow along this tube can be neglected. Due to the fact that during the

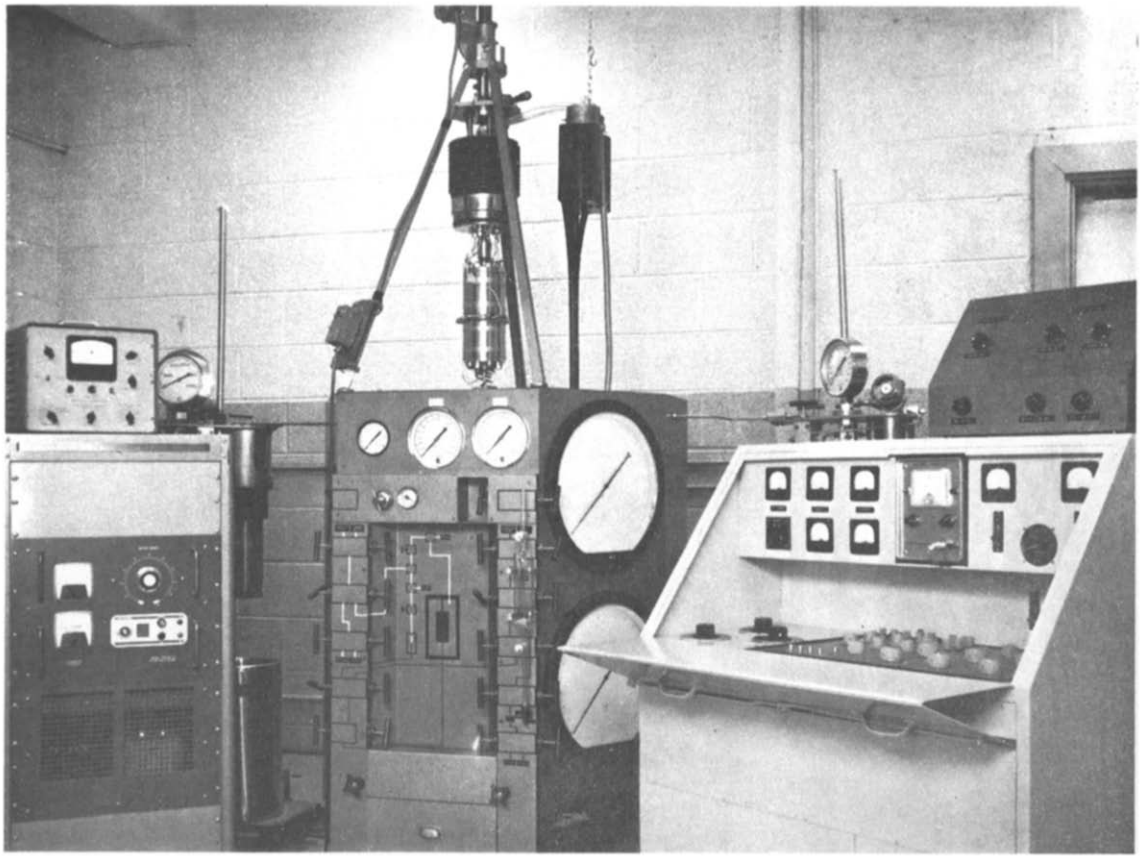

FIG. 8. Instrumentation for thermal conductivity measurements.

determination of the geometric constant the disturbance of the field at this centering location is included in the capacitance measurement the disturbance caused by the centering at the bottom can also be regarded as not existent, i.e. no corrections are needed.

Quite different is the situation at the top of the heater element where the contact to the cold body is made by the centering rod in which all lead-in wires are enclosed. The heat flow along the rod is not only governed by its thermal conductivity, its cross-sectional area and its length and ΔT, it is also a function of the thermal conductivity of the test fluid surrounding the rod in an annulus and the amount of heat dissipated in the leads which in turn is a function of the measuring conditions in the test layer.

The heat flow along the rod can be found analytically by solving the equation for temperature distribution in a thin long rod with uniformly distributed heat sources extended from a surface

$$\frac{d^2\zeta}{dx^2} = m^2\zeta - \frac{\dot{q}}{k_s} \tag{6}$$

where

$\dot{q}$ = heat generated per unit volume

$\zeta = T - T_c$

k_s = apparent thermal conductivity of the rod

$$m = \sqrt{(k)}\sqrt{\left(\frac{2\pi}{k_s A_s \ln D_a/D_i}\right)}$$

A_s = average cross-sectional area of rod

D_a, D_i = diameters of annulus formed by test fluid surrounding the rod.

The general solution of (6) is of the form

$$\zeta = M e^{-mx} + N e^{mx} + \frac{\dot{q}}{k_s m^2} \tag{7}$$

where M and N are arbitrary constants to be evaluated with the boundary conditions

$\zeta = 0$ at $x = L$

$\zeta = \zeta_o\,(T = T_h)$ at $x = 0$.

The temperature distribution is then given by

$$\zeta = \zeta_o \frac{\sinh m(L - x)}{\sinh mL} - \frac{\dot{q}}{k_s m^2} \frac{\cosh m(L/2 - x)}{\cosh mL/2} + \frac{\dot{q}}{k_s m^2}. \tag{8}$$

The temperature gradient at $x = 0$ becomes

$$\left(\frac{d\zeta}{dx}\right)_{x=0} = -m\zeta_0 \coth mL + \frac{\dot{q}}{k_s m^2} m \tanh \frac{mL}{2} \tag{9}$$

and the heat loss from the heater element is

$$q_L = k_s A_s m \left(\zeta_o \coth mL - \frac{\dot{q}}{k_s m^2} \tanh \frac{mL}{2}\right). \tag{10}$$

The heat generated per unit volume is

$$\dot{q} = \frac{I^2 R_L}{A_s L} \tag{11}$$

where R_L = resistance of the lead-in wires enclosed in the rod of length L

I = current.

Introducing constants

$$A_1 = \sqrt{\left(k_s A_s \frac{2\pi}{\ln D_b/D_i}\right)}$$

and

$$A_2 = \frac{2\pi L}{\ln D_a/D_i}$$

equation (10) becomes with (11) and after rearranging

$$q_L = \tanh \frac{mL}{2} A_1 \sqrt{(k)} \left(\zeta_o \frac{\coth mL}{\tanh mL/2} - \frac{I^2 R_L}{A_2 k}\right). \tag{12}$$

Since the current passing through the lead-in wires generates within the heater element of resistance R_h the heat I^2R_h; I^2 in equation (12) can be replaced with the aid of equation (1) and equation (12) finally yields

$$q_L = \tanh\frac{mL}{2} A_1 \sqrt{(k)} \left[\zeta_0\left(\frac{\coth mL}{\tanh mL/2} - \frac{BR_L}{A_2R_h}\right)\right]. \quad (13)$$

for all values $mL > 6$ (which can normally be achieved easily by choosing proper L and/or m) the hyperbolic functions become unity and equation (13) simplifies to

$$q_L = A_1\sqrt{(k)}\left[\zeta_0\left(1 - \frac{B \cdot R_L}{A_2R_h}\right)\right]. \quad (14)$$

For our geometry and all values of $k > 0{\cdot}000232$ Watt/cm degC equation (14) is valid.

The term BR_L/A_2R_h in equations (13) and (14) is a dimensionless number and can be written as $K = [(R_L/A_2)/(R_h/B)]$ where R_L/A_2 is the resistance of the lead-in or its loss related to the geometrical and physical conditions governing the loss; and R_h/B is a similar ratio formed with similar quantities of the system. If these two ratios are equal to each other ($K = 1$) or equal to coth mL/tanh $mL/2$, then the lead-in acts as a guard no loss will occur along it in either direction from the system. If K is larger than coth mL/tanh $mL/2$ or for large values of mL, larger than unity, additional flow into the system along the lead-in takes place. [In this case the thermal conductivity evaluated with equation (1) will be too small.]

The opposite holds true for values of K smaller than unity. Since this dimensionless number K resulted from the solution of the Poisson equation similar dimensionless numbers will describe the lead-in losses of any other similar system for which the Poisson equation is valid also.* B, A_2 and R_h are given values and known at 25°C; R_L can be chosen so that

$$\frac{B \cdot R_L}{A_2R_h} = 1$$

making the heat loss along the centering rod zero.

The geometric constant B changes with temperature, so does A_2. Since the thermal expansion coefficients of metals are small and do not differ too much from material to material, the ratio B/A_2 can be regarded as remaining constant with temperature. For the case that lead-ins and heater coil are made out of the same material the ratio R_L/R_h also would not change with temperature. The heat loss from the heater element along the centering rod therefore could be neglected for any temperatures. This ideal situation is not present in our case for several reasons. The material used for lead-ins and heater coil are different, k_s is not exactly known and A_s is an average cross-sectional area of the tapered rod and for small values of k the hyperbolic functions are not equal to unity. Furthermore, k itself might be different in the gap and the annulus due to different free convection and radiation heat transfer. Finally, the heat is generated in the lead-in wires and not uniformly in the rod. All this is of second order influence and the overall error at 25°C due to heat loss along the rod can still be regarded as being negligibly small and within the accuracy claimed. At other temperature levels and measuring fluids of very low thermal conductivity corrections can be made analytically and checked experimentally by evacuating the cell and measuring the heat input to the heater element and accounting for the radiant heat transfer through the empty gap.

3.7.2 *Temperature drop in wall.* Knowing the heat transferred from the heater element to the cold body makes it possible to evaluate the temperature drop in the metal layer between the thermocouples and the surface of the two bodies. As described in Section 3.1, the thermocouple joints are placed in good thermal contact in the center of copper tips which tightly fill the holes provided. The location of those tips within the copper walls in relation to the surfaces are well known by careful measurements. If one assumes radial heat flow the temperature drop in the walls can be estimated with the thermal conductivity of copper and the measured distances. The correction will be largest by measuring good conducting liquids, and will then be of the order of 0·3 per cent. In any case, the error resulting from uncertainty in this correction will be much smaller and might be of the order of several hundredth of a per cent. To make the error negligibly small needs perfect corrections

* See W. Leidenfrost's forthcoming publication.

and it seems to be a long way until this can be achieved. The correction for radiant heat exchange appears equally difficult as will be discussed later.

The heat dissipated in the heater element and the temperature difference are known but this is still not sufficient to calculate the thermal conductivity with the aid of equation (1) or (1a) because part of the heat might be transferred by free convection and/or radiation.

3.7.3 *Heat transfer by free convection.* In any arrangement other than a horizontal layer of test fluid heated from above free convective motion is present, no matter how small the temperature differences are. But, it has been shown that, for very slow so called "creeping motions", heat is still transferred through the fluid layer by conduction alone. For our combined geometry creeping motion exists as long as the product of the Grashof and Prandtl numbers is less than 1200. A considerably smaller value than 1200 can always be achieved by measuring liquids under almost any pressure and temperature but not at, or close to, critical point conditions where the *Gr Pr* product becomes infinite. Due to the low dynamic viscosity of gases and vapors and due to their density change with pressure free convection can be expected in a very few of them, especially at high pressures and low temperatures. In those rare cases, it is necessary to measure the thermal conductivity several times with decreasing temperature difference. Extrapolating towards zero degree temperature difference will yield the true value, but one has to keep in mind that overall error increases because the measured quantities become small.

3.7.4 *Heat transfer by radiation.** The outside of the heater element and the surface of the cavity of the cold body are gold coated and highly polished in order to minimize radiant heat exchange. To assure a lasting layer of gold an undercoat of rhodium as diffusion barrier was necessary. The gold layer was thick enough to guarantee non-porosity which is not only of importance in respect to the optical properties of the surfaces but also vital for the prevention of corrosion and for reaction of the test fluid with the copper walls causing a change in the fluid itself.

For correction for radiant heat exchange there are three distinct conditions which must be treated separately. First, the most simple case of a perfectly opaque fluid where no correction is necessary. Second, the fluid is perfectly transparent and corrections can easily be made by measuring the heat loss from the heater element when the apparatus is evacuated so highly that the mean free path of the molecules exceeds by many times the width of the gap. The conduction through the rarefied gas is then negligibly small and the heat input to the heater element after correction for the heat loss along the centering devices is equal to the heat transferred by radiation.

The third case, of partly transparent fluids capable of emitting and absorbing radiation, is much more complicated. Since most liquids and all polyatomic gases and vapors are of this kind a more thorough treatment is needed. So far, to the best knowledge of the author, only approximate solutions of this problem have been applied, but no rational adjustment of measurements of thermal conductivity of radiating fluids to allow for radiation absorption emission characteristics has ever been made.

Thermal radiation in partly transparent fluids affects the heat transfer in two ways; first, directly as in the case of perfectly transparent fluids the energy is absorbed and emitted by the surfaces of the cell; secondly, the radiation is absorbed and emitted by the test fluid altering the temperature distribution in a way that the temperature gradient across the layer of test fluid is highest near the two surfaces and smallest at some points in-between. This influences the radiant heat transfer and also the thermal conductivity because the actual temperature gradient present within the test fluid during the measurements does not correspond to that in equation (1) which was derived from Fourier's Law. The temperature distribution or the local gradient depends not only on the geometry of the system but also on the temperature of the two surfaces, radiative properties and on the

* This section has been written with the asisstance of Professor Raymond Viskanta. His help and suggestions are highly appreciated by the author.

ratio of heat transfer by conduction in comparison to that by radiation. All this makes it clear that the usual procedure of subtracting the radiant energy exchange measured in vacuum from the total energy input (measured with fluid in the gap) to the heater element is generally not permissible unless the radiation effect is smaller than the experimental error of the thermal conductivity measurements.

In order to correct the measurements for radiation the energy equation must be solved. For simultaneous conduction and radiation this equation becomes a complicated non-linear integro-differential equation. In order to make solution possible it is necessary to reduce the geometric complexities introduced by the dependence of the radiant energy flux on our test cell configuration. Therefore, in the following it is assumed that the heat transfer takes place between two infinitely large parallel plates. This assumption seems to be permissible because of the large ratio of the diameter to the width of the test layer. The physical model considered is shown in Fig. 9. The walls of the test cell are assumed to be isothermal, diffusive emitters and absorbers of thermal radiation and to have

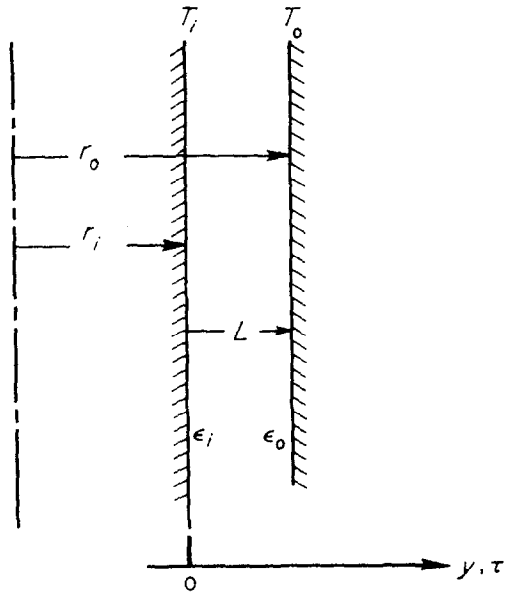

FIG. 9. Model of layer of test fluid in thermal conductivity cell.

constant radiation properties except for variation in wavelength. The fluid is supposed to be an isotropic homogeneous gas or liquid which can absorb and emit thermal radiation, and the fluid is at rest. The energy equation for this case has been solved by Viskanta and Grosh [8], and the radiation heat flux coming from the heater element at surface i and passing through a fluid having a monochromatic absorption coefficient κ_λ and an index of refraction n_λ is given as

$$q_r = 2\int_0^\infty \left[R_{0,\lambda} E_3(\tau_{0,\lambda}) + \int_0^{\tau_{0,\lambda}} n_\lambda^2(\tau_\lambda) E_{b,\lambda}(\tau_\lambda) E_2(\tau_\lambda)\, d\tau_\lambda - \tfrac{1}{2} R_{t,\lambda}\right] d\lambda \tag{15}$$

where the optical depth τ_λ is the new independent variable. τ_λ and the optical thickness $\tau_{0,\lambda}$ are defined as

$$\tau_\lambda = \int_0^y \kappa_\lambda\, dy \tag{16}$$

$$\tau_{0,\lambda} = \int_0^L \kappa_\lambda\, dy. \tag{17}$$

$E_{b,\lambda}$ is the monochromatic emissive power of a black body and $E_n(x)$ is an exponential integral function defined as

$$E_n(x) = \int_0^1 \mu^{n-2} \exp\left(-\frac{x}{\mu}\right) d\mu. \tag{18}$$

The monochromatic radiosity or radiant energy leaving the boundary at r_i is given by

$$R_{i,\lambda} = \epsilon_{i,\lambda} n_\lambda^2(0) E_{b,\lambda}(0) + 2(1 - \epsilon_{i,\lambda})\left[R_{0,\lambda} E_3(\tau_{0,\lambda}) + \int_0^{\tau_{0,\lambda}} n_\lambda^2(\tau_\lambda) E_{b,\lambda}(\tau_\lambda) E_2(\tau_\lambda)\, d\tau_\lambda\right]. \tag{19}$$

The first term on the right represents the emission by surface i. The second term gives the fraction of the incident energy that is reflected from surface i. The radiant energy incident on i is

due to radiation leaving surface 0 plus radiation emitted by the fluid.

The monochromatic hemispherical emissivity of the solid surface i is defined as the ratio of the monochromatic emissive power of surface i $E_{\lambda,i}$ to the monochromatic emissive power of a black body radiating into a fluid having an index of refraction n_λ, $\epsilon_{\lambda,i} = E_{\lambda,i}/n_\lambda^2 E_{b,\lambda}$. When $n_\lambda = 1$, this reduces to the conventional definition of the monochromatic hemispherical emissivity. Due to the lack of information, the functional dependency of the emissivity on the optical properties of the two materials involved cannot be predicted.

The energy flux leaving the surface 0 is similar to equation (19).

$$R_{0,\lambda} = \epsilon_{0,\lambda} n_\lambda^2(\tau_{0,\lambda}) E_{b,\lambda}(\tau_{0,\lambda}) + 2(1-\epsilon_{0,\lambda})\left[R_{i,\lambda} E_3(\tau_{0,\lambda}) + \int_0^{\tau_{0,\lambda}} n_\lambda^2(\tau_\lambda) E_{b,\lambda}(\tau_\lambda) E_2(\tau_{0,\lambda}-\tau_\lambda)\,\mathrm{d}\tau_\lambda\right]. \quad (20)$$

Equations (19) and (20) can be solved simultaneously and the resulting radiosities can be introduced into (15). But the evaluation of this equation is still very complex due to the double integration. To simplify the calculation it is assumed that ϵ_λ, n_λ can be replaced by appropriate average values and that the absorption coefficient is given by Planck's mean value

$$\kappa = \frac{\int_0^\infty \kappa_\lambda E_{b,\lambda}\,\mathrm{d}\lambda}{\int_0^\infty E_{b,\lambda}\,\mathrm{d}\lambda} = \frac{\int_0^\infty \kappa_\lambda E_{b,\lambda}\,\mathrm{d}\lambda}{\sigma T^4} \quad (21)$$

where σ is the Stefan–Boltzmann constant. The radiant heat flux can now be expressed as

$$q_r = 2\left[R_o E_3(\tau_o) + n^2\sigma\int_0^{\tau_0} T^4(\tau) E_2(\tau)\,\mathrm{d}\tau - \tfrac{1}{2} R_i\right]. \quad (22)$$

Making equation (22) dimensionless by introducing the variables:

$$\theta = \frac{T}{T_i}; \quad \Phi = \frac{q_r}{n^2\sigma T_i^4}; \quad \beta = \frac{R}{n^2\sigma T_i^4}$$

yields

$$\Phi = 2\left[\beta_o E_3(\tau_0) + \int_0^{\tau_0} \theta^4(\tau) E_2(\tau)\,\mathrm{d}r - \tfrac{1}{2}\beta_i\right]. \quad (23)$$

Solution of (19) and (20) yields

$$\beta_i = \frac{\epsilon_i + 2(1-\epsilon_i) I_i + 2(1-\epsilon_i)\epsilon_0\theta_0^4 E_3(\tau_0) + 4(1-\epsilon_i)(1-\epsilon_0) E_3(\tau_0) I_0}{1 - 4(1-\epsilon_i)(1-\epsilon_0) E_3^2(\tau_0)} \quad (24)$$

and

$$\beta_0 = \frac{\epsilon_0\theta_0^4 + 2(1-\epsilon_0) I_0 + 2(1-\epsilon_0)\epsilon_i E_3(\tau_0) + 4(1-\epsilon_i)(1-\epsilon_0) E_3(\tau_0) I_i}{1 - 4(1-\epsilon_i)(1-\epsilon_0) E_3^2(\tau_0)} \quad (25)$$

where

$$I_i = \int_0^{\tau_0} \theta^4(\tau) E_2(\tau)\,\mathrm{d}\tau \quad (26)$$

and

$$I_0 = \int_0^{\tau_0} \theta^4(\tau) E_2(\tau_0 - \tau)\,\mathrm{d}\tau. \quad (27)$$

Thus if the temperature distribution is known the radiant heat-transfer rate can be predicted.

In general $\theta(\tau)$ could be found from the solution of the conservation of energy equation and would yield a temperature profile as discussed above. However, it has been found that when the parameter

$$N = \frac{\kappa \cdot k}{4\sigma T^3} > 10 \quad (28)$$

the temperature distribution is very little affected by the presence of radiation and is governed by conduction alone. This also holds true for the case when the optical thickness $\tau_0 < 0{\cdot}1$. For the computed results given below either or both of these conditions were satisfied and therefore the temperature distribution used in evaluating the radiant heat flux is

$$\theta(\tau) = 1 + \frac{\tau}{\tau_0}(\theta_0 - 1). \quad (29)$$

This linear temperature distribution can be still regarded as being correct [9] even for cases when

the above conditions are not perfectly met for cases where $T_i \approx T_0$ as it will be always in the experiments.

Substituting (29) into (26) and (27) and integrating gives

$$I_i = \tfrac{1}{2} - E_3(\tau_0) + \frac{4}{\tau_0}(\theta_0 - 1)\left[\tfrac{1}{3} - \tau_0 E_3(\tau_0) - E_4(\tau)\right] + \frac{6}{\tau_0^2}(\theta_0 - 1)^2\left[\tfrac{1}{2} - \tau_0^2 E_3(\tau_0) - 2\tau_0 E_4(\tau_0) - 2E_5(\tau_0)\right] \quad (30)$$

and

$$I_0 = \tfrac{1}{2} - E_3(\tau_0) + \frac{4}{\tau_0}(\theta_0 - 1)\left[-\tfrac{1}{3} + \frac{\tau_0}{2} + E_4(\tau_0)\right] + \frac{6}{\tau_0^2}(\theta_0 - 1)^2\left[-\tfrac{1}{2} + \frac{\tau_0^2}{2} - \frac{2\tau_0}{3} - 2E_5(\tau_0)\right]. \quad (31)$$

Since the temperature difference by measuring the thermal conductivity always will be small $(\theta_0 - 1)$ is small and therefore terms containing $(\theta_0 - 1)^3$ and $(\theta_0 - 1)^4$ have been neglected in (30) and (31). Equation (23) can now be solved for the radiant heat exchange, but the calculation is still somewhat involved and it is therefore of interest to discuss further a more simple approach and check how well it compares with the exact method.

It has been known for some time that if the optical thickness of radiating matter is large, i.e. $\tau_0 \gg 1$, the radiant energy flux can be considered as a diffusion process. The radiant heat flux at points optically far from the walls in case of gray radiating fluids can be represented by the equation

$$q_r = -k_r \frac{\mathrm{d}T}{\mathrm{d}y} \quad (32)$$

where the radiative conductivity k_r is given by

$$k_r = \frac{16 n^2 \sigma T^3}{3\kappa_r}$$

and the Rosseland mean free path of radiation is defined as [10]

$$\frac{1}{\kappa_r} = \frac{\int_0^\infty \frac{1}{\kappa_\lambda}\frac{\mathrm{d}E_{b,\lambda}}{\mathrm{d}y}\,\mathrm{d}\lambda}{\int_0^\infty \frac{\mathrm{d}E_{b,\lambda}}{\mathrm{d}y}\,\mathrm{d}\lambda} \cdot \frac{\int_0^\infty \frac{1}{\kappa_\lambda}\frac{\mathrm{d}E_{b,\lambda}}{\mathrm{d}y}\,\mathrm{d}\lambda}{\frac{\mathrm{d}}{\mathrm{d}y}(\sigma T^4)}. \quad (33)$$

The diffusion approximation works well in the interior of a fluid, but is not accurate near boundaries because it does not take into account radiation leaving the surfaces. Thus, except for extremely large optical thicknesses (high pressure in radiating gases) considerable error may be made in the calculations of radiant heat transfer through a fluid for given temperature of the boundary surfaces.

The range of validity of the diffusion approximation has been extended by introducing the jump boundary conditions at the walls. This has been done by Shorin [11] and more recently by Probstein [12] and Deissler [13] by different methods.

Using Deissler's approach the validity of the diffusion approximation can be extended to radiating fluids having an index of refraction different from unity. The equation for radiant heat flux can then be expressed as

$$q_r = \frac{n^2(E_{b,i} - E_{b,0})}{\frac{3}{4}\tau_r + (1/\epsilon_i) + (1/\epsilon_0) - 1} \quad (34)$$

with $\tau_r = \kappa_r L$. In the limiting case of $n = 1$ equation (34) reduces to

$$q_r = \frac{E_{b,i} - E_{b,0}}{\frac{3}{4}\tau_r + (1/\epsilon_i) + (1/\epsilon_0) - 1} \quad (35)$$

as it has been shown by Deissler.

Equation (35) differs somewhat from the equation given by Shorin; in his equation the first term in the denominator is 4/3 times higher than that given in (35). This is due to the fact that k_r used by Shorin was 4/3 times smaller than that used by Deissler. Comparisons show [12, 13] that equation (35) predicts radiant heat-transfer rates that are in good agreement with the numerical solutions of the exact integral equation for all values of optical thickness in the case when the walls of the system are black. It should also be remembered that equation (34) has been derived by assuming that heat transfer by conduction was absent.

With the aid of equations (23) and (34) the radiant heat exchange has been evaluated. Since the optical properties used for calculations are not known precisely, it seemed to be permissible tc use throughout $\tau_0 = \tau_r$.

The calculation shows that the diffusion approximation yields larger values of radiant heat exchange than using the exact approach. q_r in each case [as easily can be seen from equations (23) and (34)] decreases with increasing optical thickness. This decrease is more rapid when the radiant heat transfer is calculated from the energy equation, therefore the difference in q_r obtained by the two methods increases with increasing optical thickness. These results are of interest to thermal conductivity measurements for the following reasons. If thermal conductivity data for absorbing media are not corrected for radiant heat exchange they will show a dependence on the thickness of the test layer and also on pressure, the latter especially for gases or vapors. Increasing the thickness and/or the pressure will result in an apparent decrease of thermal conductivity. Therefore equally precise determinations of thermal conductivity carried out in different instruments will disagree with each other, maybe only due to the fact that the geometry used was different or the pressure was not the same (assuming k is independent of pressure) and therefore the radiant heat exchange influences the measurements by a different amount. The dependence of thermal conductivity on test layer thickness is noticeable in the results published by Fritz and Poltz [14]. Thermal conductivity of liquids not corrected for radiant heat exchange shows quite clearly a decrease with increasing thickness of the test layer. (For water that decrease seems to be larger than one would expect from the calculations). The decrease in thermal conductivity is with further increase of test layer thickness first compensated and later overcompensated by free convection. Fritz and Poltz also observed a dependence on the temperature difference under which the measurements had been carried out, even in the region where no free convection was noticeable. The higher values of k observed in the case of larger temperature differences cannot be explained by radiant heat exchange because the calculation of the error caused by radiation is practically independent of the temperature difference, at least for values of one and five degrees. This is noticeable in Figs. 10, 11 and 12 where ratios of radiant to total heat transfer through a stagnant parallel layer of toluene, water and water vapor respectively are plotted versus temperature. These ratios have been calculated from equations (23) and (34) using thermal conductivity and optical property data listed in handbooks. The optical data are normally given only for one temperature. For other conditions they were corrected, or in the case of the spectral distribution of the absorption coefficient, it was assumed to be constant with temperature. This introduces a certain degree of uncertainty which, however, can be expected to be small.

Fig. 10 shows how much thermal conductivity measurements on toluene are influenced by radiant heat transfer. If the walls of the instrument have an emissivity of 0·1 then at room temperature the error is approximately 0·1 per cent and increases to 0·2 per cent at boiling temperature. For the same temperature range the error changes from 1 to 2 per cent when the walls of the conductivity cell are black. If no corrections for radiant heat exchange are applied to the measurements the values of thermal conductivity will be too high by the same percentages. If the thermal conductivity data are corrected by using the diffusion approximation the resulting values will be too small by an amount of 0·5–1 per cent for black walls and 0·1–0·5 per cent for walls having an emissivity of 0·1 and for the temperature range given. These results seem to be of special importance because toluene has been recommended as a calibration or control fluid for thermal conductivity measurements [15, 16]. If one investigator attempts to correct his results by using the diffusion approximation then he overcorrects and his results will deviate from the exact value almost as much but only in the opposite direction as when no correction was made. Therefore, the disagreement between otherwise equally precise measurements becomes larger. This stresses the fact that in some cases the more involved exact correction must be used. A similar situation is given for water (Fig. 11) but the influence of radiant heat exchange on thermal conductivity measurements is much smaller, due

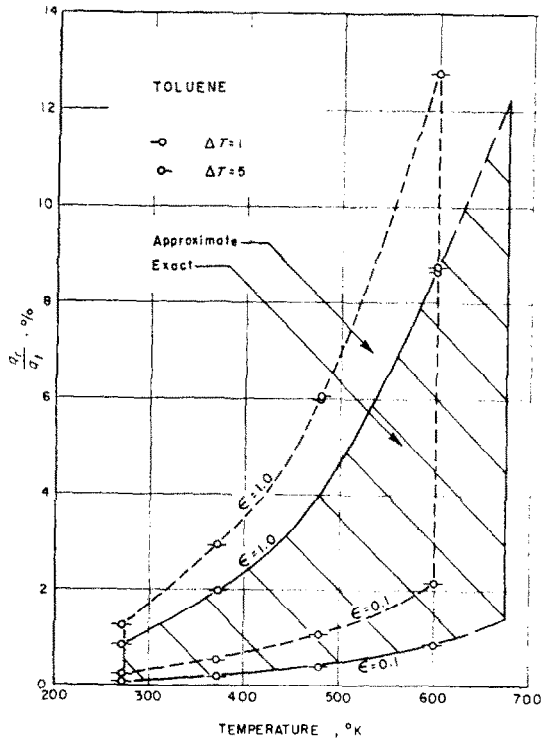

FIG. 10. Ratio of radiant to total heat transferred through a stagnant layer of toluene between parallel walls.

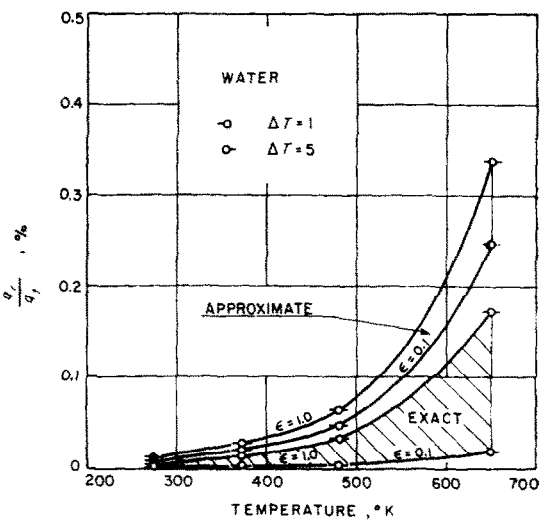

FIG. 11. Ratio of radiant to total heat transferred through a stagnant layer of water between parallel walls.

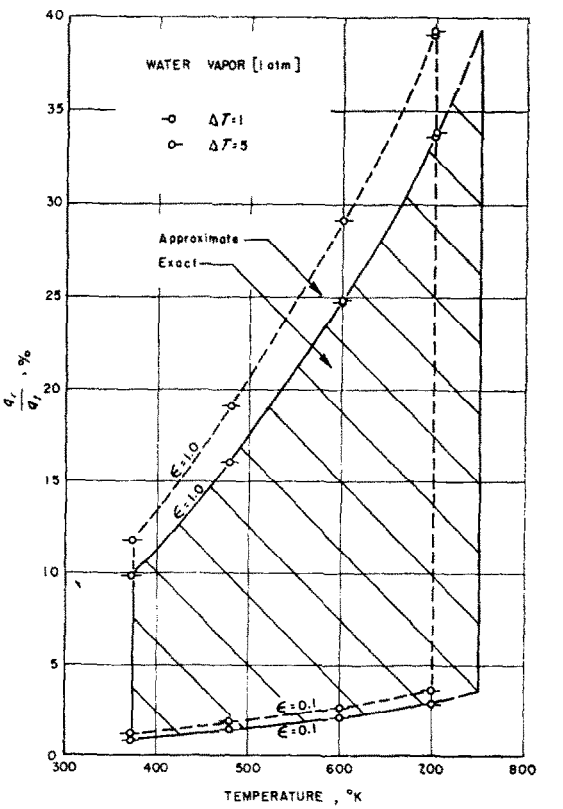

FIG. 12. Ratio of radiant to total heat transferred through a stagnant layer of water vapor [1 atm] between parallel walls.

to its more than twenty times larger optical thickness and also due to its higher thermal conductivity compared with the properties of toluene. For water vapor, as shown in Fig. 12, the radiant heat exchange at 1 atm is considerably larger. Increasing the vapor pressure will increase the optical thickness and therefore in high pressure steam the radiant heat exchange might be of the same order of magnitude as in the case of toluene and water, but the influence of increase in optical thickness could be compensated by an increase in the index of refraction. Due to the lack of information, calculations could not be made.

Summarizing, it can be stated that errors on thermal conductivity measurements introduced by radiant heat exchange cannot always be assumed to be negligibly small even for fluids which appear to be very opaque. In order to achieve high accuracy, corrections should be made but this might often be impossible be-

cause the optical properties are not known. Therefore, it is essential to make and to keep the surfaces of the walls of thermal conductivity cell as mirrorlike as possible. The surface material should be selected properly also in respect of its porosity and chemical and physical stability under measuring conditions. Furthermore, one has to keep in mind that the radiant heat exchange measured in the instrument under vacuum not necessarily yields the true emissivity values for the correction of thermal conductivity measurements due to the influence of the index of refraction of the test fluid which is not only of importance for fluids able to absorb and emit radiation but also for perfectly transparent fluids if their refractive index deviates considerably from unity as it can at high temperatures and pressures.

4. EXPERIMENTAL RESULTS

4.1. *Thermal conductivity of helium over a range of pressure*

There are several reasons to select helium as first substance to be measured with the conductivity cell. The viscosity of helium shows a negative pressure dependence as measured by Kestin and Leidenfrost [3]. This decrease with pressure cannot be explained theoretically and therefore it seemed to be of interest to check if the thermal conductivity is influenced by pressure in a similar way which should be the case because both properties are dependent on the intermolecular forces in a similar manner. This expectation is in disagreement with thermal conductivity measurements by Johannin, Wilson and Vodar [17]. Their results show an increase of thermal conductivity with pressure which is rather steep in the region where the decrease of viscosity has been observed and becomes less at higher pressures. This initial large pressure dependence becomes more noticeable at higher temperatures. Other reasons for selecting helium are due to its simple molecular structure making theoretical prediction of its properties more probable. Furthermore, helium has a value of thermal conductivity which is approximately in the middle of possible values of all common fluid media. In addition, helium has an index of refraction close to unity even at high pressures and finally under these conditions the product of $Gr\,Pr$ is several hundred times smaller than its critical value, assuming therefore that free convection heat transfer will not influence the measurements.

The results are represented in Fig. 13, where the thermal conductivity at 17·4°C is plotted against pressure for the range from 1 atm to 120 atm. Two curves obtained during the present work are shown and for comparison Johannin's data are given in a third curve. Furthermore, viscosity values are included in the figure. The values measured first are represented by the dotted line. In a second run repeated measurements obtained under increasing and decreasing pressure are give by the full line. The helium used during the investigation is a product of Air Reduction Company, New York, N.Y., and has a purity of 99·989 per cent.

The storage tank was connected to the system as described in Section 3.6. For the first test the instrument was evacuated by means of the vacuum system connected to the main instrument unit by means of a 2 cm i.d. copper pipe and the valves shown in Fig. 5. After the pressure in the 2 cm pipe was kept for several hours below 1 μ the cell was filled with helium, evacuated again but for a shorter period and refilled. This cycle was repeated several times. Measurements began at atmospheric pressure. Subsequent readings under increasing pressure indicated a very steep increase of thermal conductivity at the low pressure end and a sharp change of the slope at moderate pressures. Further pressure increase finally caused an almost linear pressure dependence of thermal conductivity, having a gradient approximately equal to that observed by Johannin at higher pressures. Decreasing the pressure from 100 atm to 1 atm produced an almost linear decrease in thermal conductivity over the total range. (These values are not included in the figure in order to avoid interference with the data measured during the second run.) These inconsistent results could be explained only by impurities (air and water vapor) causing even in a very small concentration due to their low thermal conductivity a noticeable decrease of the high thermal conductivity of helium.

Following the layout in Fig. 5 explains how impurities could have remained in the cell despite

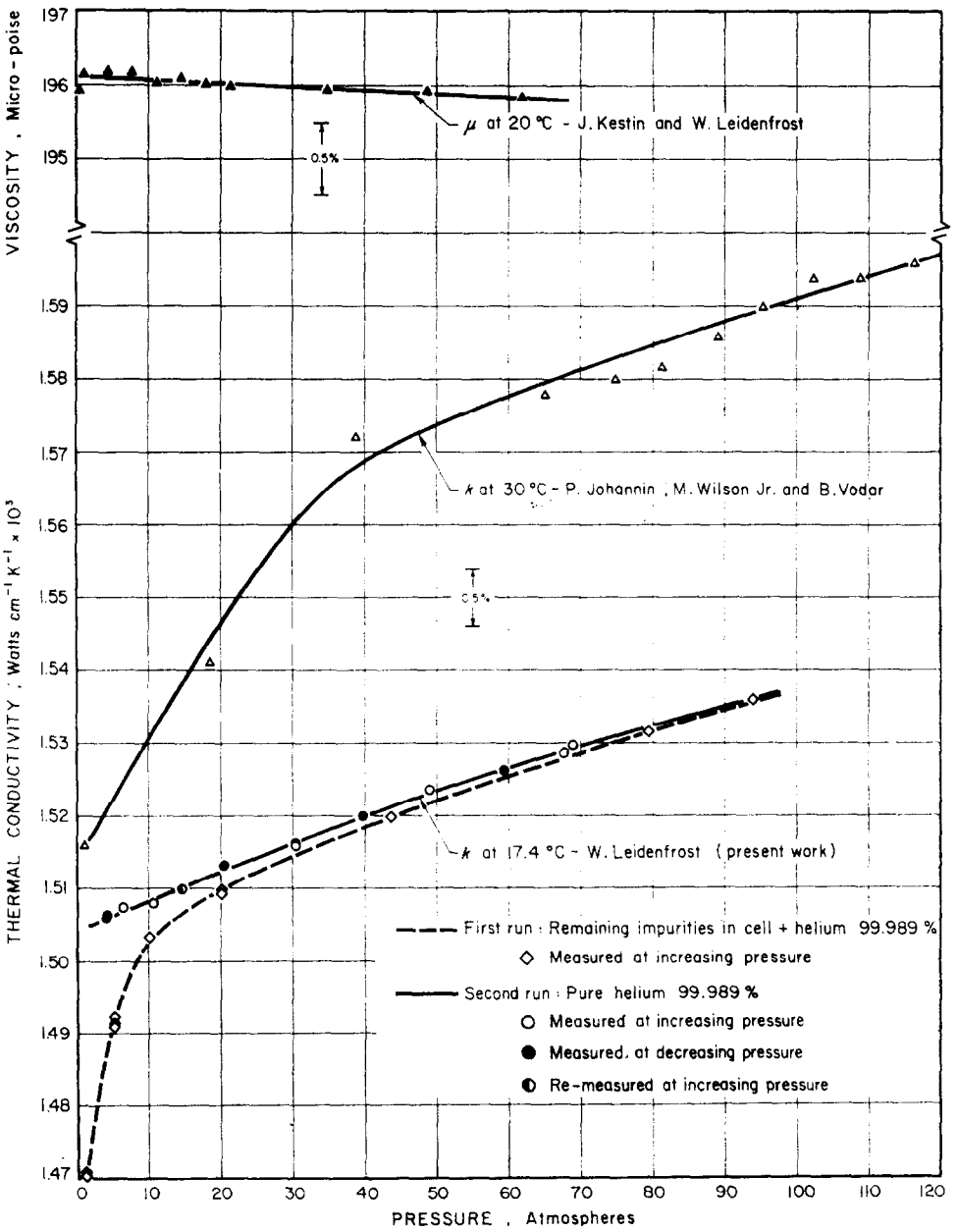

FIG. 13. The thermal conductivity and the absolute viscosity of helium at different temperatures plotted against pressure.

the precautions followed to avoid them. The cell itself is at the end of the high pressure line and also at the end of the vacuum line. Evacuating the cell by means of the fairly wide copper line does not necessarily empty the cell at the same time down to the same pressure as observed in the copper tube because in the high pressure line Knudsen flow exists slowing down the evacuation process considerably. Therefore at the end of this process there was still a certain amount of gas inside the cell. During the filling this gas is not removed, it remains inside the instrument and there are also added the impurities which remained in the high pressure lines. Increasing the pressure by adding more helium into the cell will only decrease the concentration of impurities. In case water vapor was present, this decrease would occur very rapidly until all vapor is condensed. Further pressure increase will then result in a lesser linear decrease of impurity concentration. The curve measured during the first run demonstrates this condition quite clearly. To assure complete removal of all impurities for the second run the instrument was evacuated again, but for a longer time at higher temperatures of the cell and the instrument was filled with high pressure helium. After allowing sufficient mixing time the helium was drained out of the cell until 1 atm was reached. This cycle was repeated at least ten times. During the last cycle the cold body temperature was decreased to its final value which was then maintained constant for all measurements. Readings were taken under increasing pressure up to 70 atm then under decreasing pressure to the lowest value and finally a further point was measured by increasing the pressure again. The curve obtained in this way is covered by thirteen points fairly evenly spaced. The measured values scatter from the smooth curve by several hundredths of a per cent. An attempt was made to measure the pressure dependence of thermal conductivity of helium at 20°C. The regulating device to hold the cold body temperature constant failed unfortunately and it was necessary to maintain the instrument at tap water temperature, by means of the water bath. In addition tap water was also forced through the cooling coil. This water did run first to the coil placed within the water bath in order to damp very small temperature fluctuations. This precaution made fast temperature fluctuations unnoticeable but creeping changes of temperature level could not be eliminated completely, resulting in a very slow oscillation of the cold body temperature with an amplitude of a few thousandths of a degree. When the direction of temperature change reversed there was sufficient time to reach steady state not under perfect conditions but good enough for taking final readings. The small scatter of the experimental points from the smooth curve might be partly caused by the above-mentioned oscillation. For all measurements the temperature difference between the cold body and heater element was kept practically constant. It was chosen to be large enough that it could be measured with high accuracy. After completion of the second run the instrument was evacuated in order to evaluate the radiant heat exchange, which was very small and can be assumed to be constant for the correction of all the thermal conductivity data measured because not only the temperature difference was the same but also the refractive index did practically not deviate from unity.

The smooth curve shows an almost linear pressure dependence in the pressure range 1–30 atm. In the neighborhood of 30–40 atm the gradient begins to decrease. This decrease continues but lessens with further pressure increase. For the thirteen measurements taken during the second run approximately 14 h were needed. If the cold body is maintained definitely at a constant temperature steady state can be reached much faster and the values obtained will be of less scatter and more accurate.

The overall absolute accuracy can be assumed to be of the order of 0·1 per cent. The largest error is due to uncertainties in measuring the temperatures of the heater element and cold body. For the continuation of the work k as function of pressure and temperature of helium, carbon dioxide, water and toluene, will be measured next.* The thermostating device as well as the temperature measurement techniques will be improved so that equally

* See W. Leidenfrost's forthcoming publication.

precise or even more accurate data can be obtained.*

The author is aware of the fact that the accuracy claimed is unusually high for thermal conductivity measurements. For this reason it seems to be worthwhile to discuss briefly the errors influencing thermal conductivity measurements and the steps possible to avoid or reduce them. Fourier's Law in its simplest form relates the heat flow directly to the thermal conductivity, the area and the temperature difference between the heat source and the heat sink and inverse to the thickness of the test layer. This equation is quite misleading for thermal conductivity measurements because perfect conditions rarely exist and many corrections are necessary. For the heat flow one has to correct for radiant heat exchange, heat transport by free convection, lead-in losses which can be in either direction and for errors introduced by temperature fluctuations coming from the cold body or the heat source and are of different influence. Corrections also might be needed for inhomogeneities within the heat source and sink, and within the test fluid. A similarly large number of corrections must be applied to the area, thickness and temperature difference, or the temperatures.

Avoiding and/or correcting most of the errors is insufficient if steady state cannot be achieved and maintained long enough to take the readings. In an instrument as used in the present work this necessary condition can be much more easily achieved than in apparatus using guard heaters, the same can be said about the uniformity in the temperature field. In addition, it was shown that the heat loss along the lead-in rod can be made very small and even negligibly small by designing it properly. The area and thickness measured combinedly by determining the capacitance of the arrangement is by far superior than by measuring them separately because all fringe effects are included and finding the setting for minimum capacity assumes best homogeneity. (This is especially important in the case of horizontal layers because a change in thickness will result also in a change of effective area due to changing inhomogeneities.) The cold body designed as a thermostat and the good thermal contact of the heater coil (being itself like a solid body of high thermal conductivity) assures to a high degree uniform heating and therefore uniform temperature distribution. For all those mentioned reasons the accuracy claimed and possible to reach in the future seems not to be too optimistic. Also for the additional reason that heat exchange by radiation can be predicted more precisely by solving the energy equation and by the possibility to measure one of the important properties for radiant heat exchange simultaneously in the same instrument by determining the dielectric constant of the test fluid.

* A platinum resistance thermometer is being built into the cold body for automatically regulating the cold body temperature and also for the calibration of the thermocouples in the cell.

4.2. *Dielectric constant*

The geometric constant of the cell configuration had been determined as outlined in Sect. 3.2. by measuring the capacitance under vacuum. Repeating the capacitance measurements when the instrument is filled with the test fluid allows the dielectric constant of the test material to be calculated with the known geometric constant and the aid of equation (2).

This has been done with three materials of the highest purity: argon, carbon dioxide and toluene. The results are given in Table 1. For comparison NBS values listed in circular 537 [18] for 20°C and 1 atm have been corrected for the same temperature and pressure conditions as our measurements by using equation (36) recommended by NBS in circular 537 and valid for temperatures 10–30°C and pressures 700–800 mm Hg.

$$\frac{(\epsilon - 1)_{T,p}}{(\epsilon - 1)_{20^\circ\mathrm{C},\,1\,\mathrm{atm}}} = \frac{p}{760\,[1 + 0{\cdot}003411\,(T - 20)]}. \tag{36}$$

Toluene was measured at room temperature but the temperature of the cell was not determined accurately enough to allow corrections.

The excellent agreement of the measured values with the recommended ones proves that despite repeated dismantling and assembling the geometric constant of the cell is reproducible

Table 1. *Dielectric constant of several test fluids of highest purity measured under normal conditions*

Material	Argon	CO_2	Toluene
Temp.°C	25.04	24.00	——
Press.,mm Hg	746.76	755.14	——
ϵ(measured)	1.0004932	1.000899	2.3787
N. B. S. value corrected for the same temp. & press.	1.0004996	1.0009038	2.379 (not corrected)
Departure	−6 ppm	−5 ppm	——

The measurements furthermore indicate that the three lead capacitance measurement was done properly, since when there was still a lead-in capacity included in the measurements this part would have not been changed by filling the test layer with a fluid therefore introducing larger deviations in the results.

5. OUTLOOK AND DISCUSSION OF A MULTIPURPOSE INSTRUMENT

Whoever needs values of properties for any theoretical or technical purpose finds himself in a dilemma the instant he starts searching the literature. Normally one may be able to find the value of one property given at certain conditions. In some cases this one property even might be listed as function of temperature, pressure, etc. But very often the ranges covered do not include those needed. Finding values of a second property of the same substance for the conditions wanted happens not too often. Searching for values of a third, fourth, etc., property for the same ranges is in most cases a hopeless task. The situation is worsened by the fact that the different values given have not necessarily been observed with the same substances, even when nominally the material tested is called the same.

To improve the situation by measuring all properties over the widest possible ranges is, as we know, impractical. But, as already discussed, the task becomes less tremendous by selecting specific test substances and measuring selected properties of most utility to theoretical research. The task appears to become even more promising and feasible by developing multipurpose instruments able to produce data for several properties simultaneously. The thermal conductivity cell discussed in the previous sections of this paper could easily be redesigned and some of its special features improved in such a way that over the same or wider ranges of pressure and temperature the following properties can be measured.

1. Thermal conductivity k.
2. Electrical conductivity λ.
3. Power factor, dielectric constant ϵ and therefore index of refraction n.
4. p-v-T properties of gases or vapors and hence the compressibility factor.
5. Vapor pressure of liquids.
6. The thermal expansion coefficient of the test cell material.

Such a multipurpose instrument could be similar to our thermal conductivity cell. Applying an electrical potential difference between heater element and cold body and measuring the current flowing through the test fluid allows the determination of the electrical conductivity with the aid of the equation (1) due to similarity of the electrical and thermal field. For determination of the dielectric constant the same arrangement as we had could be used but special design is necessary to make three lead capacitance measurements possible without interfering with the detection of emf's and power input. Measur-

ing the capacitance of the arrangement under vacuum at different temperatures produces the geometric constant as a function of temperature and this in turn gives the thermal expansion of the test cell material and hence the true volume occupied by the test fluid within the instrument. Therefore the apparatus can be used for p-v-T measurements. (A similar pressure measuring device as shown in Fig. 7 but more sensitive would then be used and the overall volume would be increased by adding another cavity for making the observations more feasible.)

Measuring the capacitance of the arrangement filled with the test fluid together with the value observed under vacuum gives the dielectric constant and hence the refractive index. Balancing the capacitance bridge yields also the power factor.

From a study of the variation of k, ϵ, p, v with T an analysis can be made of the intermolecular potential function most accurate in presenting the observed temperature variations for moderate pressure. For higher pressure the variation of properties can be used to check dense gas theory. From the potential function other properties such as diffusion coefficient, viscosity, etc., can be calculated. If ideal gas thermodynamic data are available (or if they can be calculated from spectroscopic data) the above measurements can be used to generate enthalpy, entropy, specific heats, free energy, etc., thermodynamic functions.

The properties measured will have been obtained for an identical sample under identical conditions so that no error will occur in comparing experimental data measured in different apparatus for different temperatures, pressures and impurity contents. Moreover, the additional expenses of multiple instruments, operation costs, supplies, etc. are eliminated.

It might be possible to extend the use of the instrument further and it is certainly possible to build other multipurpose instruments measuring several other properties. This should enable a more rapid determination of many properties of selected substances to be made and such detailed property data will then be useful for checking the validity of existing theories and therefore could make the prediction of data more accurate.

ACKNOWLEDGEMENTS

The work described in this paper was jointly sponsored by the National Science Foundation under Contract NSF G-17455 and by the United States Army Research Office under Contract DA-31-124-ARO(D)-40 with Purdue University. The funds granted made possible the whole investigation and is gratefully acknowledged. The author wishes to express his gratitude to Mr. H. Wagemann, former technician at the Forschungsinstitut für Verfahrenstechnik Aachen, whose skill and painstaking work made it possible to solve many problems arising during the design of the instrument. The author also is grateful to Mr. H. Langemeier who built the cell at the Institute of Thermodynamic and Heat Transfer at the Technische Hochschule Braunschweig and who was always willing to modify and especially to rebuild one major part of the instrument in a short time period in 1962 after it was damaged accidentially. The success of this investigation was made possible by the cooperation of several graduate students and staff members at Purdue University. Mr. C. Y. Ho assisted in assembling the overall instrumentation in performing the measurements and preparing the drawings. Mr. P. Lall performed the calculations of the errors introduced by radiant heat exchange.

The work at Purdue was supported in the beginning by Mr. W. Cole and for the last two years by Mr. R. Kemp. Both contributed materially to the success of this investigation by their skill as mechanics. Finally the author wishes to extend his gratitude to all these colleagues especially for their patience in not getting frustrated whenever the very good work of today was redone tomorrow just for the sake of possible improvements.

REFERENCES

1. P. E. LILEY, Survey of recent work on the viscosity, thermal conductivity and diffusion of gases and gas mixtures, thermodynamic and transport properties of gases, liquids and solids, *ASME*, New York, 40–69 (1959).
2. P. E. LILEY, Survey of recent work on the viscosity, thermal conductivity, and diffusion of gases and liquefied gases below 500°K. Progress in International Research on Thermodynamic and Transport Properties, *ASME*, New York, 313–339 (1962).
3. J. KESTIN and W. LEIDENFROST, An absolute determination of the viscosity of eleven gases over a range of pressures, *Physica*, **25**, 1033–1062 (1959).
4. J. KESTIN and W. LEIDENFROST, The viscosity of helium, *Physica*, **25**, 537–555 (1959).
5. E. SCHMIDT und W. LEIDENFROST, Der Einfluss elektrischer Felder auf den Wärmetransport in flüssigen elektrischen Nichtleitern, *Forsch. Ing. Wes.* **19**, 65–80.
6. E. SCHMIDT und W. LEIDENFROST, Wärmeleitzahl-Messungen an Wasser, Äthylenglykol-Wasser-Mischungen und Kalziumchlorid-Lösungen im Temperaturbereich von 0 bis 100°C, *Forsch. Ing.-Wes.* **21**, 176–180 (1955).

7. W. LEIDENFROST, Messung der Wärmeleitzahl von Milch mit verschiedenem Wassergehalt im Temperaturbereich von 20° bis 100°C, Fette-Seifen-Anstrichmittel-Die Ernährungsindustrie, **61**, 1005–1010 (1959).
8. R. VISKANTA and R. J. GROSH, Heat transfer by simultaneous conduction and radiation in an absorbing medium, *Trans. ASME, J. Heat Transfer*, **84C**, 63–72 (1963).
9. R. VISKANTA, Heat transfer in Couette flow of a radiating fluid with viscous dissipation. Proceedings of the 8th Midwestern Mechanics Conference, 1–3 April 1963, Pergamon Press (in press).
10. S. ROSSELAND, *Astrophysik und Atomtheoretische Grundlage*, pp. 41–44. Springer Verlag, Berlin (1931).
11. S. N. SHORIN, Heat exchange by radiation in the presence of absorbing medium, *IZV. Akad. Nauk SSSR, Otd. Tekh. Nauk*, No. 3, 389–405 (1951). [Abridged English translation in the *Engineer's Digest*, **12**, 324–328 (1951).]
12. R. F. PROBSTEIN, Radiation slip, *AIAA J.* **1**, 1202–1204 (1963).
13. R. G. DEISSLER, Diffusion approximation for thermal radiation in gases with energy jump boundary condition, *ASME* Paper No. 63-HT-13.
14. W. FRITZ und H. POLTZ, Absolutbestimmung der Wärmeleitfähigkeit von Flüssigkeiten—I, Kritische Versuche an einer neuen Plattenapparatus, *Int. J. Heat and Mass Transfer* **5**, 307–316 (1962).
15. L. RIEDEL, *Chem.-Ing.-Tech.* **23**, 321–324 (1951).
16. H. ZIEBLAND, The thermal conductivity of toluene, new determinations and an appraisal of recent experimental work, *Int. J. Heat Mass Transfer* **2**, 273–279 (1961).
17. P. JOHANNIN, M. WILSON JR. and B. VODAR, Heat conductivity of compressed helium at elevated temperatures. Progress in International Research on Thermodynamic and Transport Properties, *ASME*, New York, 418–433 (1962).
18. National Bureau of Standards, Table of dielectric constants and electric dipole moments of substances in the gaseous state. NBS Circular 537 (1953).

Résumé—On décrit une nouvelle cellule de conductibilité thermique utilisant un cylindre avec extrémités hémisphériques dans une cavité de même forme. On a employé un pont de capacités de haute précision pour déterminer la géométrie de la cellule. Les propriétés diélectriques étaient donc aussi mesurables. La configuration du thermostat permet d'obtenir de larges gammes de températures avec une erreur faible. On décrit un capteur de pression spécial fonctionnant à la température de l'essai. On a fait une analyse détaillée des erreurs provenant des pertes le long des dispositifs de centrage et de celles dues à la convection et au rayonnement. Les premières ont été éliminées à l'aide d'un nouveau nombre sans dimension. On a comparé les pertes par rayonnement approchée et exacte. La précision expérimentale est estimée à 0,1 pour cent. On a donné des résultats préliminaires pour la constante diélectrique de l'argon, du gaz carbonique et du toluène et pour la conductibilité thermique de l'hélium. Les valeurs de la constante diélectrique sont en accord avec les valeurs recommandées avec une différence relative de 6.10^{-6}. L'écart très faible autour d'une courbe lisse montre la précision élevée des valeurs de la conductibilité thermique. On suggère des modifications possibles pour pouvoir obtenir les valeurs de propriétés supplémentaires à partir d'une seule détermination, qui sont également importantes pour les théories de mécanique statistique.

Zusammenfassung—Es wird eine neue Wärmeleitzahlapparatur beschrieben bei der ein senkrecht stehender zylindrischer Heizkörper mit halbkugeligen Enden von einem gleichgeformten Hohlraum umgeben ist. Die Konstruktion und der Aufbau der Messanordnung und die Massnahmen zur Vermeidung von Messfehlern werden ausführlich behandelt. Die geometrische Konstante der Apparatur wird mit Hilfe einer Präzisions Kapazitäts Messbrucke bestimmt und damit wird auch die Messung dielektrischer Grössen möglich. Die Apparatur selbst ist als Thermostat für einen weiten Temperaturbereich und grosse Temperatur Konstanthaltung entworfen. Eine spezielle Einrichtung, die unter Versuchstemperatur arbeitet, wird für Druckmessungen beschrieben. Fehler durch Wärmeverluste durch Leitung länges der Zentrierungen, durch Konvektion und Strahlung werden analysiert. Erstere können durch die Einführung einer neuen dimensionslosen Kenngrösse eliminiert werden. Strahlungsverluste berechnet nährungsweise und exakt werden verglichen. Die Versuchsgenauigkeit wird auf 0·1% geschätzt. Vorläufige Ergebnisse werden angegeben für die Dielektrizitätskonstante von Argon, Kohlendroxyd und Toluol und die Wärmeleitzahl von Helium. Die Werte der Dielektrizitätskonstanten stimmen mit Tafelwerten bis auf 6 ppm überein. Die sehr Kleine Streuungen der Versuchswerte um eine Kurve demonstriert die hohe Genauigkeit der Wärmeleitzahlmessungen. Änderung der Versuchseinrichtung werden empfohlen, die es ermöglichen zusätzliche Stoffgrössen gleichzeitig zu bestimmen, was auch für Theorien der statistischen Mechanik von Wichtigkeit ist.

Аннотация—Описывается новое устройство для измерения теплопроводности, состоящее из вертикального цилиндра с полусферическими концами, помещенного внутри

такого же цилиндра. Подробно описана конструкция, сборка, а также способы уменьшения погрешностей. Для определения формы устройства использовался мостик емкости высокой точности, что давало возможность измерить также диэлектрические характеристики. Конструкция термостата допускает температурные изменения в широких пределах с небольшой погрешностью. Описан также специальный датчик давления, работающий при температуре эксперимента. Проведен подробный анализ ошибок при определении потерь вдоль центрирующих устройств, а также на конвекцию и излучение. Конвекция учитывается безразмерной величиной. Сравниваются приближенные и точные потреи на излучение. Точность эксперимента составляла 0,1%. Приводятся предварительные данные о значениях диэлектрической постоянной аргона, двуокиси углерода и толуола, а также теплопроводности гелия. Значения диэлектрической постоянной согласуются с рекомендуемыми данными с точночтью до 0,000006. Небольшой разброс данных на кривой показывает высокую точность значений теплопроводности. Предлагаются различные модификации для получения на основании одного измерения дополнительных характеристических величин, также представляющих интерес для теорий статистической механики.